OAK RIDGE NATIONAL LABORATORY LIBRARIES
3 4456 0548303 6

CENTRAL RESEARCH LIBRARY
DOCUMENT COLLECTION

ORNL-3723
UC-25 – Metals, Ceramics, and Materials
TID-4500 (36th ed.)

IMPACT RESISTANCE OF FUELED GRAPHITE SPHERES FOR PEBBLE-BED REACTOR APPLICATIONS

C. O. Smith
J. M. Robbins

OAK RIDGE NATIONAL LABORATORY
operated by
UNION CARBIDE CORPORATION
for the
U.S. ATOMIC ENERGY COMMISSION

CENTRAL RESEARCH LIBRARY
DOCUMENT COLLECTION
LIBRARY LOAN COPY
DO NOT TRANSFER TO ANOTHER PERSON
If you wish someone else to see this document, send in name with document and the library will arrange a loan.

LEGAL NOTICE

This report was prepared as an account of Government sponsored work. Neither the United States, nor the Commission, nor any person acting on behalf of the Commission:

A. Makes any warranty or representation, expressed or implied, with respect to the accuracy, completeness, or usefulness of the information contained in this report, or that the use of any information, apparatus, method, or process disclosed in this report may not infringe privately owned rights; or

B. Assumes any liabilities with respect to the use of, or for damages resulting from the use of any information, apparatus, method, or process disclosed in this report.

As used in the above, "person acting on behalf of the Commission" includes any employee or contractor of the Commission, or employee of such contractor, to the extent that such employee or contractor of the Commission, or employee of such contractor prepares, disseminates, or provides access to, any information pursuant to his employment or contract with the Commission, or his employment with such contractor.

ORNL-3723

Contract No. W-7405-eng-26

METALS AND CERAMICS DIVISION

IMPACT RESISTANCE OF FUELED GRAPHITE SPHERES FOR PEBBLE-BED REACTOR APPLICATIONS

C. O. Smith and J. M. Robbins

JANUARY 1965

OAK RIDGE NATIONAL LABORATORY
Oak Ridge, Tennessee
operated by
UNION CARBIDE CORPORATION
for the
U. S. ATOMIC ENERGY COMMISSION

OAK RIDGE NATIONAL LABORATORY LIBRARIES

3 4456 0548303 6

CONTENTS

	Page
Abstract	1
Introduction	3
Impact Resistance of Solid Graphite	3
Specimens and Test Methods	3
Comparison of Grades of Graphite	4
Effect of Drop Height	6
Effect of Specimen Size	9
Variation in Properties	11
Effect of Density on Properties	11
Effect of Thermal Cycling	15
Failures and Damage Region	15
Impact Resistance of Fuel Elements	22
Specimens and Test Methods	22
Effect of Design and Fabrication Variables	25
Other Concepts	32
Conclusions	36
Recommendations for Future Investigations	37
Appendix	39

IMPACT RESISTANCE OF FUELED GRAPHITE SPHERES FOR PEBBLE-BED REACTOR APPLICATIONS

C. O. Smith[1] and J. M. Robbins

ABSTRACT

Graphite fuel spheres for on-stream fueling of gas-cooled reactors of the pebble-bed type must withstand repeated drops. A program to develop a fuel sphere to meet the requirements for the German Pebble-Bed Reactor (AVR) focused attention on the machined-shell concept in which a premolded spherical fuel insert [containing pyrolytic-carbon-coated $(Th,U)C_2$ particles in a graphite matrix] is cemented in a premachined, fully graphitized, unfueled shell. Two studies were undertaken: (1) evaluation of impact resistance of commercially available graphite for the shell and (2) determination of the minimum shell thickness required and the effect of insert-shell gaps, which could be present initially or develop during reactor operation.

In the initial study, 1.5-in.-diam spheres, machined from four grades of extruded graphite and four grades of molded graphite, were dropped from 13 m onto a steel plate until failure. Grade ATJ graphite was clearly the best and was used almost exclusively in further tests.

The results of free-drop tests on ATJ graphite show:

1. Impact resistance decreases as drop height increases.
2. Impact resistance depends on specimen size with best resistance in the smallest specimens.
3. Impact resistance varies from one block to another with no correlation between impact resistance of a given sphere and its original position in the block.
4. Bulk-density variations between 1.65 and 1.80 g/cm^3 have no effect on impact resistance.
5. All damage occurs within the outer 7/16 in. of 6-cm-diam spheres.
6. Thermal cycling in vacuum can have an adverse effect while similar cycling in helium or hydrogen has none.

Results of drop-weight tests substantiate the conclusions derived from free-drop tests.

---

[1]Education Division.

In the fueled-sphere tests, simulated elements (the fueled portion simulated by a sphere of solid CS-312 graphite) were dropped from 4 m onto a bed of graphite spheres until failure or 75 drops, whichever was less, followed by dropping of surviving elements from 4 m onto a steel plate to failure. The results are:

1. The effects of preassembly cleaning and variations in plug-closure torques between 15 and 50 in.-lb and in types of cements (P-514, C-10, and Hexalon) are negligible.
2. Elements with uncemented inserts are clearly inferior to elements with completely cemented inserts.
3. Shells with 0.8-cm-thick walls are satisfactory for nominal radial clearances between insert and shell of 0.005 to 0.010 in., but 1.0- to 1.2-cm-thick shells would be required for clearances of 0.020 to 0.025 in.

INTRODUCTION

Graphite fuel spheres for on-stream fueling of gas-cooled reactors of the pebble-bed type must withstand repeated drops. For example, the tentative specifications for the AVR state that, after 10 thermal cycles in vacuum between room temperature and 1000°C, each 6-cm-diam fuel element must be able to sustain 50 drops from a height of 4 m (13.1 ft) onto a close-packed bed of 6-cm-diam solid graphite spheres three layers deep. A program to develop a fuel sphere to meet these and other AVR requirements focused attention on the machined-shell concept in which a premolded spherical fuel insert [containing pyrolytic-carbon-coated $(Th,U)C_2$ particles in a graphite matrix] is cemented in a premachined, fully graphitized, unfueled shell with a threaded plug. Two related courses of investigation were undertaken to develop this concept: (1) evaluation of impact resistance of commercially available graphite for the shell and (2) determination of the minimum shell thickness required and the effect of insert-shell gaps, which could be present initially or develop during reactor operation.

IMPACT RESISTANCE OF SOLID GRAPHITE

Four grades of extruded (TSX, AGOT, CS-312, and HLM-85) and four grades of molded (C-18, 9050, 3499-S, and ATJ) graphite, all commercially available, were considered for use as shell material. Grade HLM-85 graphite is produced by Great Lakes Carbon Company, grades 3499-S and 9050 graphites by Speer Carbon Company, and the other five grades by Carbon Products Division of Union Carbide Corporation.

Specimens and Test Methods

All specimens were machined as solid spheres from graphite available in Oak Ridge from stock obtained by normal purchase. Three types of tests were performed:

1. In the free-drop test, the sphere was dropped from the desired height onto a 2-in.-thick steel plate bolted to a concrete pad. Orientation of the specimen from one drop to the next was completely random.

2. In the drop-weight test, the sphere was placed on a steel plate, and a weight was dropped onto the graphite sphere. Five different weights were available, and the drop height could be varied within the limits of the machine. Different weight-height combinations appear to have no effect on failure, provided the kinetic energy of the weight at impact is constant. Orientation of the specimen from one drop to another was completely random. Although the free drop is similar to operating conditions, the drop-weight test was developed for convenience and better control of irradiated material during hot-cell evaluation. For correlation with free-drop tests, the kinetic energy of the dropped weight at impact was the same as that of the freely dropped sphere at impact.

3. In the crushing test, the sphere was crushed between two flat steel plates in a universal testing machine. Orientation of the molding, or extrusion, direction in the sphere was completely random relative to the direction of loading.

The tentative specifications for AVR fuel elements state:

> "Any chipping in excess of 1/8-in in greatest lateral dimension or a depth exceeding 1/16-in, or cracking shall be considered a failure. Cracks are defined as a linear-type defect which cannot be removed without causing rejection by other criteria as cited above for chips."

In our tests, any defect visible to the naked eye was considered a failure. This criterion is only slightly more rigorous than the AVR specifications.

Comparison of Grades of Graphite

Four grades of extruded graphite (TSX, AGOT, CS-312, and HLM-85) and four grades of molded graphite (C-18, 9050, 3499-S, and ATJ) were considered. Spheres of 1.5-in. diam were machined from all grades and tested by all three methods.

The results of free-drop tests from 13 m (42.6 ft) are shown in Fig. 1. Results of drop-weight and crushing tests are shown in Figs. 19 and 20 in the appendix. The length of the vertical line through the plotted point indicates the spread in the data. The greater spread in data for the molded graphites, especially ATJ, is at least partly due to the fact that spheres were taken along the center lines of relatively small (4-in. diam) extrusions, whereas spheres were taken from several places in the cross section of relatively large molded pieces (e.g., ATJ blocks are 9 × 20 × 24 in.). Grade ATJ graphite is clearly the best in

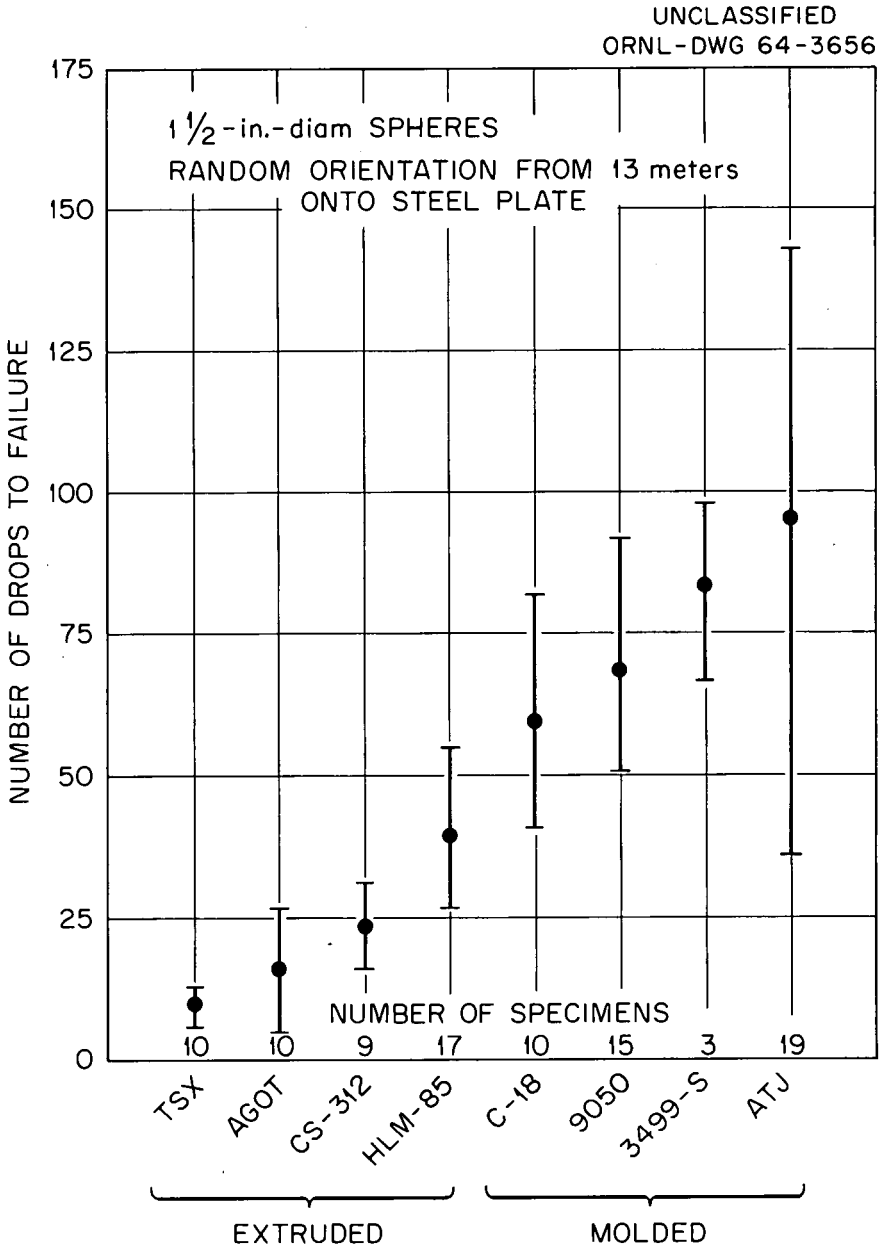

Fig. 1. Comparison of Number of Drops for Failure in Free-Drop Tests.

resistance to free-drop impact although slightly inferior to 9050 in drop-weight impact resistance and crushing load. On the basis of tests and availability, ATJ was used almost exclusively in further tests.

The relationship between crushing strength and free-drop impact resistance is shown in Fig. 2. The squares around each plotted point indicate the spread in the data. The relationships between crushing strength and drop-weight impact resistance and between free-drop and drop-weight impact resistance are shown in Figs. 21 and 22 in the appendix.

Effect of Drop Height

The stresses produced by pressure between two spheres as a result of impact or static load are given by Timoshenko and Goodier,[2] based on original work by Hertz,[3] assuming the spheres are isotropic and elastic. The maximum tensile stress occurs at the circular boundary of the surface of contact and is radial to this boundary. The plate is a sphere of infinite mass and radius for impact between a sphere and a flat plate. The maximum tensile stress developed in a sphere dropped from a height, h, onto a flat plate of another material is given by

$$\sigma_r = \frac{2(1 - 2\nu_1)\ (2.5\pi h\rho)^{1/5}}{3\pi\left(\frac{1 - \nu_1^2}{E_1} + \frac{1 - \nu_2^2}{E_2}\right)^{4/5}}\ , \qquad (1)$$

where ρ is the density of the sphere, ν is Poisson's ratio, E is Young's modulus, and subscripts 1 and 2 refer to sphere and plate, respectively.

If we assume the number of drops for failure varies inversely as the maximum load (load assumed directly proportional to stress), then the number of drops for failure would vary as $(1/h)^{0.2}$. The effect of free-drop height on impact resistance is shown in Fig. 3 in which the number of drops for failure varies approximately as $(1/h)^{1.5}$ between 5- and 13-m drop height. The number of drops from 27.3 m (89.5 ft) is lower than predicted by $(1/h)^{1.5}$ although a set of nine spheres required 3 to 10 drops for failure. The number of drops for failure in drop-weight tests with kinetic

---

[2]S. Timoshenko and J. N. Goodier, Theory of Elasticity, 2nd ed., pp. 372–384, McGraw-Hill, New York, 1951.

[3]H. Hertz, J. Reine u Angew. Math. (Crelle's) 92, 156–71 (1881).

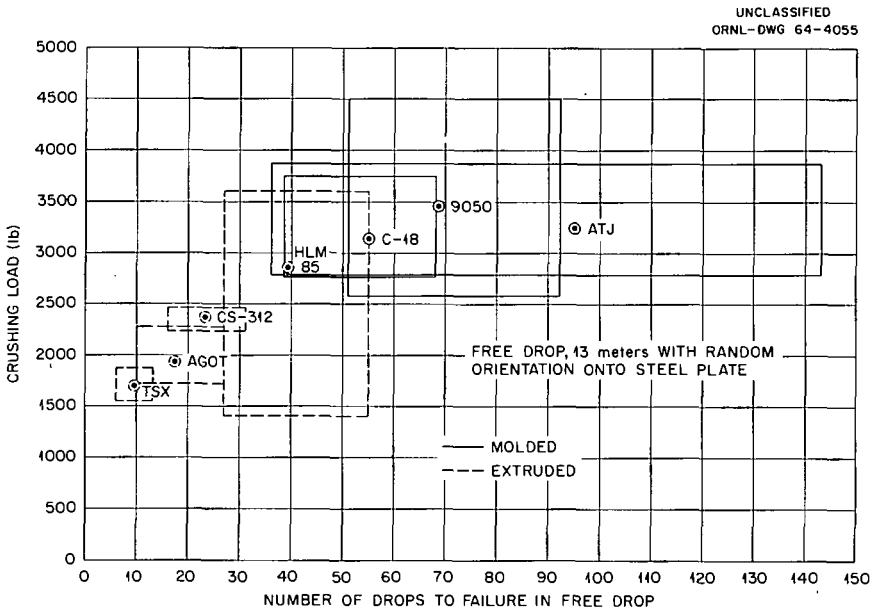

Fig. 2. Relationship Between Free-Drop Resistance and Crushing Strength of Seven Graphites; 1 1/2-in.-diam Solid Spheres.

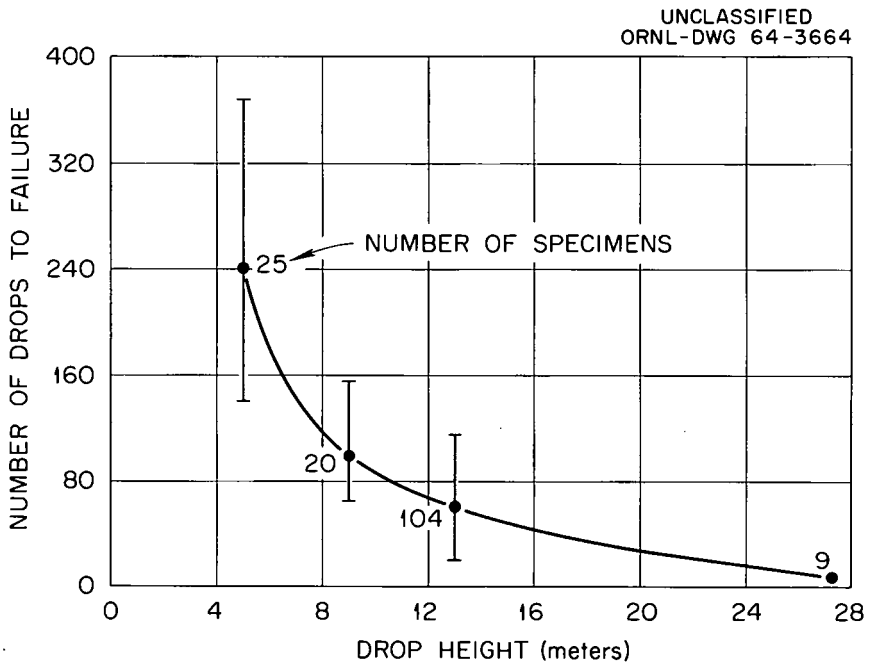

Fig. 3. Free-Drop Tests of 6-cm-diam Solid Spheres of ATJ Graphite. Effect of drop height on impact life; impact on steel plate.

energy ranging from 2.61 to 7.83 ft-lb/in.^{3} of sphere varies approximately as $(1/h)^{1.2}$. The effects of kinetic energy and momentum on impact failure in drop-weight tests are shown in Figs. 23–26 in the appendix.

Effect of Specimen Size

Equation (1) predicts that maximum tensile stress is independent of sphere size. Yahr and Smith[4] have shown (for spheres dropped from a constant height or crushed under direct loading) that the ratio of maximum forces is given by

$$\frac{P_A}{P_B} = \left(\frac{R_A}{R_B}\right)^2 . \qquad (2)$$

Thus we might expect impact resistance to be independent of sphere size.

The data from free-drop tests, shown in Fig. 4, clearly indicate a size effect with smaller spheres requiring more drops for failure than larger ones. Drop-weight tests (6-cm-diam spheres) with a constant kinetic energy of 2.61 ft-lb/in.^{3} of sphere (Fig. 28 in appendix) give a similar relationship. Direct crushing tests (Fig. 29 in appendix) also give a similar relationship between nominal stress and diameter. A log-lot plot of load vs diameter for the crushing tests is essentially linear and indicates the exponent in Eq. (2) is approximately 1.5 rather than 2. However, the free-drop and drop-weight data do not give even approximately straight lines in log-log plots.

Free-drop, drop-weight, and crushing tests of 1.5-in.-diam and 6-cm-diam spheres of HLM-85 and 9050, plus free-drop tests of 1.5-in. diam and 6-cm-diam spheres of CS-312 and AGOT, show similar behavior in these grades of graphite.

Equations (1) and (2) assume isotropy and elasticity. The lack of application of these equations in all three types of tests is at least partly due to the anisotropy and nonelasticity of graphite. The more drastic lack of application to free-drop and drop-weight tests is presumed due to the assumption of number of drops for failure varying inversely as the maximum load or stress. Data from drop-weight tests of 1.5-in.-diam spheres,

---

[4]G. T. Yahr and J. S. Smith, GCRP Semiann. Progr. Rept. Sept. 30, 1963, ORNL-3523, pp. 291–296.

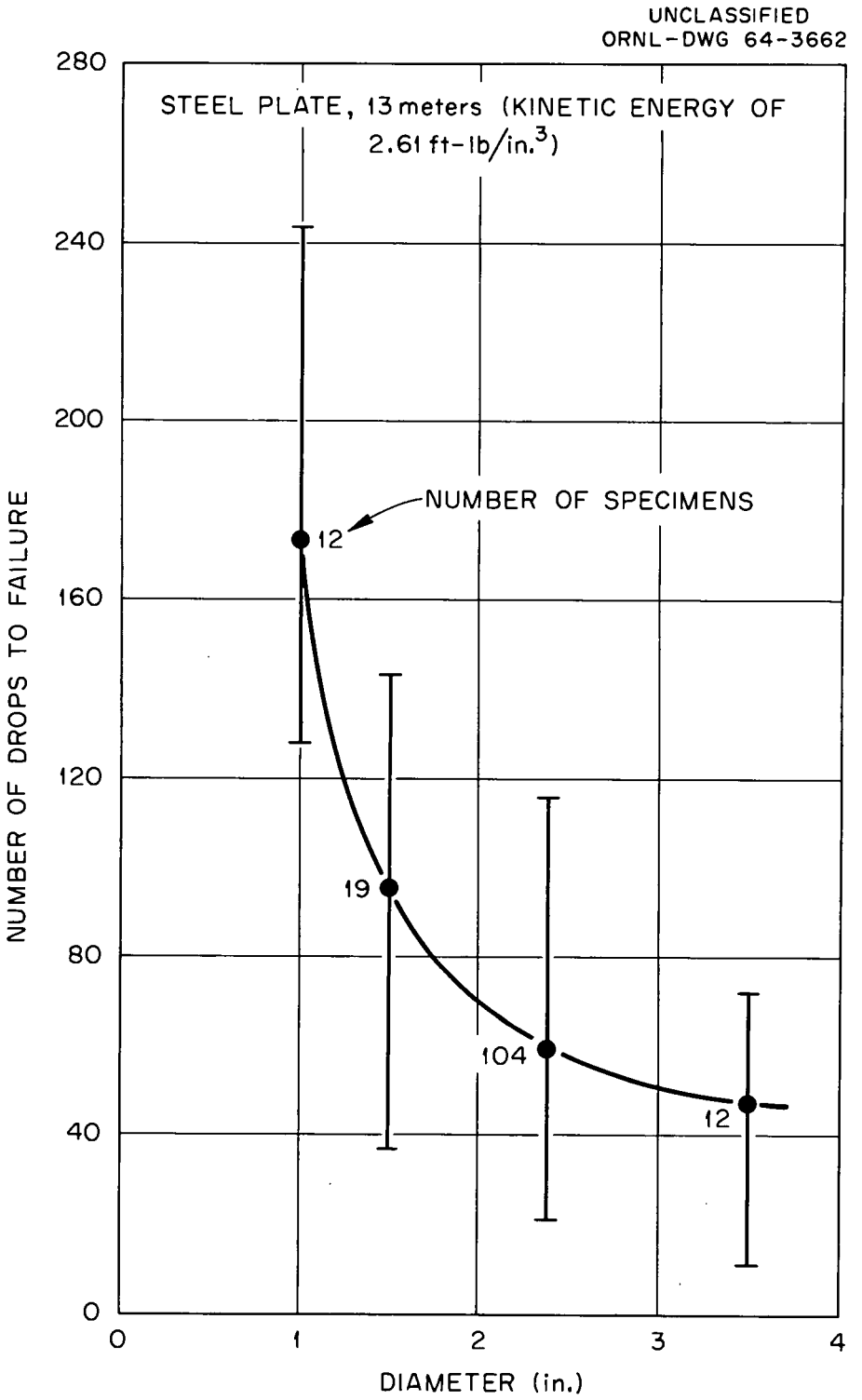

Fig. 4. Effect of Sphere Size on Number of Drops for Failure in Free-Drop Tests of ATJ Graphite Spheres.

however, show that the relationship between drops for failure and maximum force (as measured by a transducer) does not depart greatly from a linear one (Fig. 30 in appendix).

Variation in Properties

It is well recognized that graphite varies considerably in its properties. Impact resistance is no exception. Figure 5 shows the variation from one lot to another and the spread within a lot for 11 lots of ATJ graphite tested by free drop using randomly selected spheres from each lot. Similar data for drop-weight and crushing tests are shown in Figs. 31 and 32 in the appendix.

It is also well recognized that graphite has considerable variation in properties within a given piece, especially in ones of the size of ATJ blocks (9 × 20 × 24 in.). This variation normally has some relationship to position; that is, mechanical properties are lower in the center than on the surface. Spheres taken from seven blocks of ATJ were tested by all three procedures with sphere position in the block known. Figure 6, for one of these blocks, is typical. There is no discernible pattern between resistance to a test of a given sphere and the position in the block from which it was taken. While superior performance in one test generally indicates superior performance in a different test, this is not always true. One block, for example, lowest on the basis of free-drop and crushing tests, was fourth best on the basis of drop weight.

Effect of Density on Properties

Variations in bulk density of graphite, with major material and manufacturing factors being reasonably constant, are usually reflected in mechanical property variations. Bulk density was measured on a large number of ATJ spheres and varied from 1.65 to 1.80 g/cm^3. Figure 7, which shows the relationship between bulk density and free drops for failure, indicates that impact resistance does not depend on bulk density. This is supported by similar data from drop-weight and crushing tests (Figs. 33 and 34 in appendix).

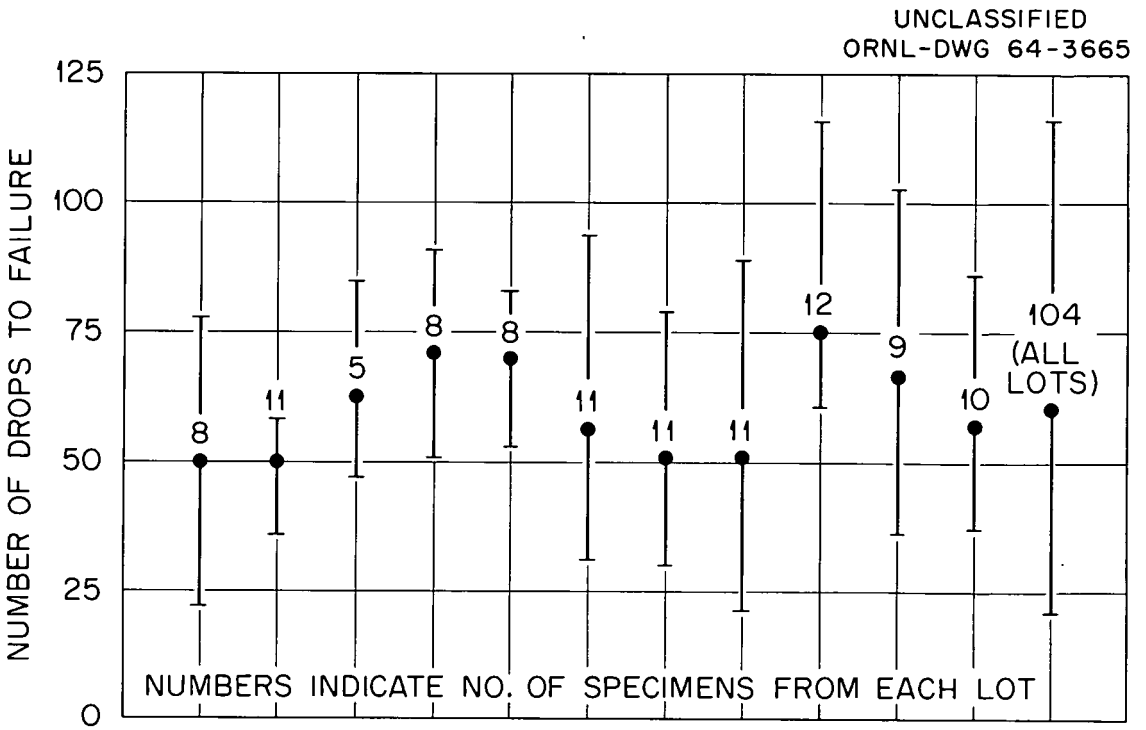

Fig. 5. Variation in Failure in Free-Drop Tests. Eleven lots of ATJ graphite; 6-cm-diam solid sphere dropped with random orientation from 13 m onto steel plate.

UNCLASSIFIED
ORNL DWG. 64-3655

VARIATION IN IMPACT AND CRUSHING BEHAVIOR OF ATJ 6 cm DIAMETER SPHERES TAKEN IN POSITIONS INDICATED FROM ONE SIDE OF A MOLDED BLOCK

F.D.	D.W.	CRUSH	F.D.	D.W.	CRUSH	F.D.	D.W.
39	82	6290 lb	55	100	6810 lb	59	63
D.W.	CRUSH	F.D.	D.W.	CRUSH	F.D.	D.W.	CRUSH
79	5560 lb	62	67	6180 lb	21	61	6000 lb
CRUSH	F.D.	D.W.	CRUSH	F.D.	D.W.	CRUSH	F.D.
5810 lb	21	64	6730 lb	74	73	6300 lb	89

F.D. – NO. OF DROPS WITH RANDOM ORIENTATION FROM 13 meters ONTO STEEL PLATE FOR FAILURE.

D.W. – NO. OF DROPS OF 12.13 lb WEIGHT THROUGH 17 7/8 in. (18.07 ft-lb) (2.61 ft-lb/in.^{3} OF SPHERE) FOR FAILURE.

Fig. 6. Variation in Impact and Crushing Behavior of 6-cm-diam ATJ Graphite Spheres Taken in Positions Indicated from One Side of a Molded Block.

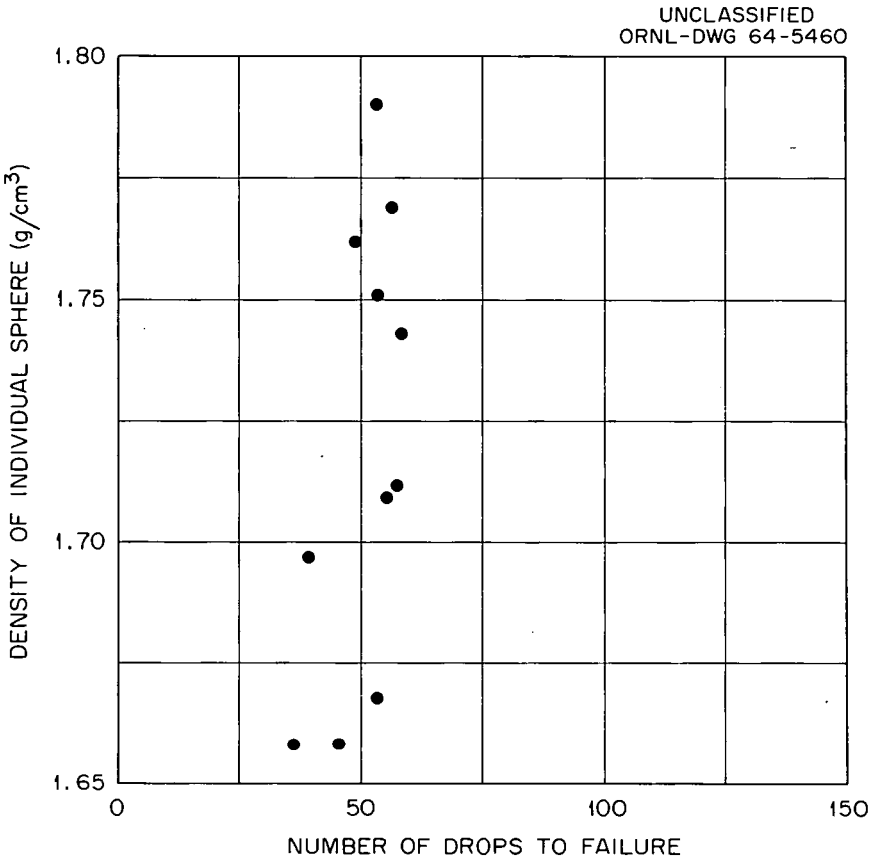

Fig. 7. Relationship Between Density and Drops for Failure in Free-Drop Tests of 6-cm-diam Solid ATJ Graphite Spheres onto Steel Plate from 13 m.

Effect of Thermal Cycling

A fuel element in the AVR will undergo thermal cycling during its normal circulation in and out of the reactor core. Thermal cycling before testing, as required by the specifications, was intended primarily as a conditioning treatment. Use of vacuum, rather than helium (which is the cooling gas in the reactor), was arbitrary since no effect on the graphite itself was anticipated. Both free-drop and drop-weight tests of spheres that had 10 thermal cycles in vacuum (1 μ Hg) between room temperature and 1000°C showed a definite loss in drops for failure and in crushing strength, as shown in Table 1. In addition, there was some change in the visual appearance of the failures. Similar thermal cycling in helium caused no change in properties or appearance of the failures using all three tests.

Later drop-weight tests of another lot of graphite showed no effect of thermal cycling in vacuum. Figure 8 compares the first lot (in the middle) with all lots (on the left) and the second lot (on the right). Spheres from this second lot were also given one thermal cycle in hydrogen between room temperature and 1000°C (the "bakeout" cycle to be discussed in the section on fuel elements). This cycle in hydrogen also had no effect on the impact resistance. Results of thermal cycling on free-drop and crushing tests are shown in Figs. 35 and 36 in the appendix.

It appears that thermal cycling in vacuum can, but will not always, decrease impact resistance of ATJ. The lack of change in visual appearance and a weight loss of approximately 0.01% after cycling in vacuum substantially eliminate the possibility of oxidation (from residual oxygen) or gas removal decreasing impact resistance. In addition, ATJ, heated in air for 30 min at 500°C with a weight loss of approximately 0.03% and some change in appearance, has no loss in impact resistance. Similar treatment at 600°C, with a weight loss of approximately 0.75% does decrease impact resistance. The first lot was below average in impact resistance while the second was slightly above average. We suspect the difference in effect of thermal cycling may be related to this difference in virgin properties.

Failures and Damage Region

Typical free-drop (13 m) test failures of ATJ are shown in Fig. 9. These ranged from (a) a small crack, through (b) a larger crack, through

Table 1. Effect of Thermal Cycling[a] in Vacuum on One Lot of ATJ Graphite[b]

	Number of Specimens	Minimum	Average	Maximum
Crush Test (Load, lb)				
Thermally cycled	10	5320	5920	7260
Virgin	9	5620	6210	7950
Virgin (all lots)	104	2600	6620	9960
Free-Drop Test, 13 m, Steel Plate (Drops to Failure)				
Thermally cycled	10	27	43.7	65
Virgin	8	22	50.0	78
Thermally cycled (2 lots)	14	27	46.4	72
Virgin (all lots)	104	21	59.7	116
Drop-Weight Test, 18.07 ft-lb[c] (Drops to Failure)				
Thermally cycled	10	37	55.8	78
Virgin	10	42	66.6	87
Virgin (all lots)	110	26	77.8	161

[a]Ten cycles from room temperature to 1000°C in vacuum (1 μ Hg).
[b]Solid spheres 6 cm in diameter.
[c]Equivalent to 2.61 ft-lb/in.^{3} of sphere.

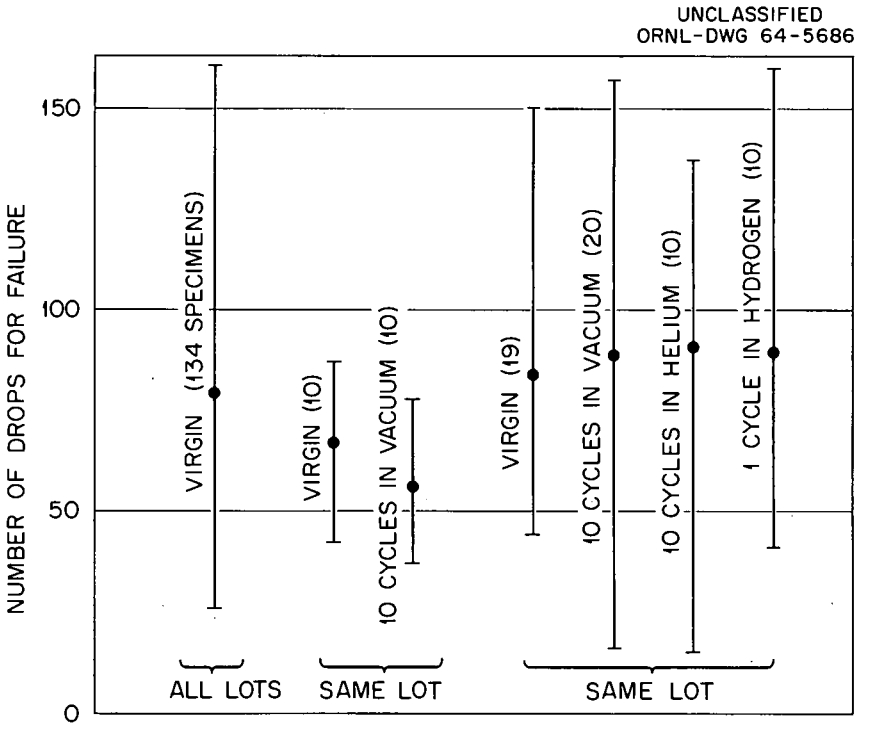

Fig. 8. Effect of Thermal Cycling from Room Temperature to 1000°C on Failure in Drop-Weight Tests (2.61 ft-lb/in.^{3} of Sphere) of 6-cm-diam ATJ Graphite Spheres.

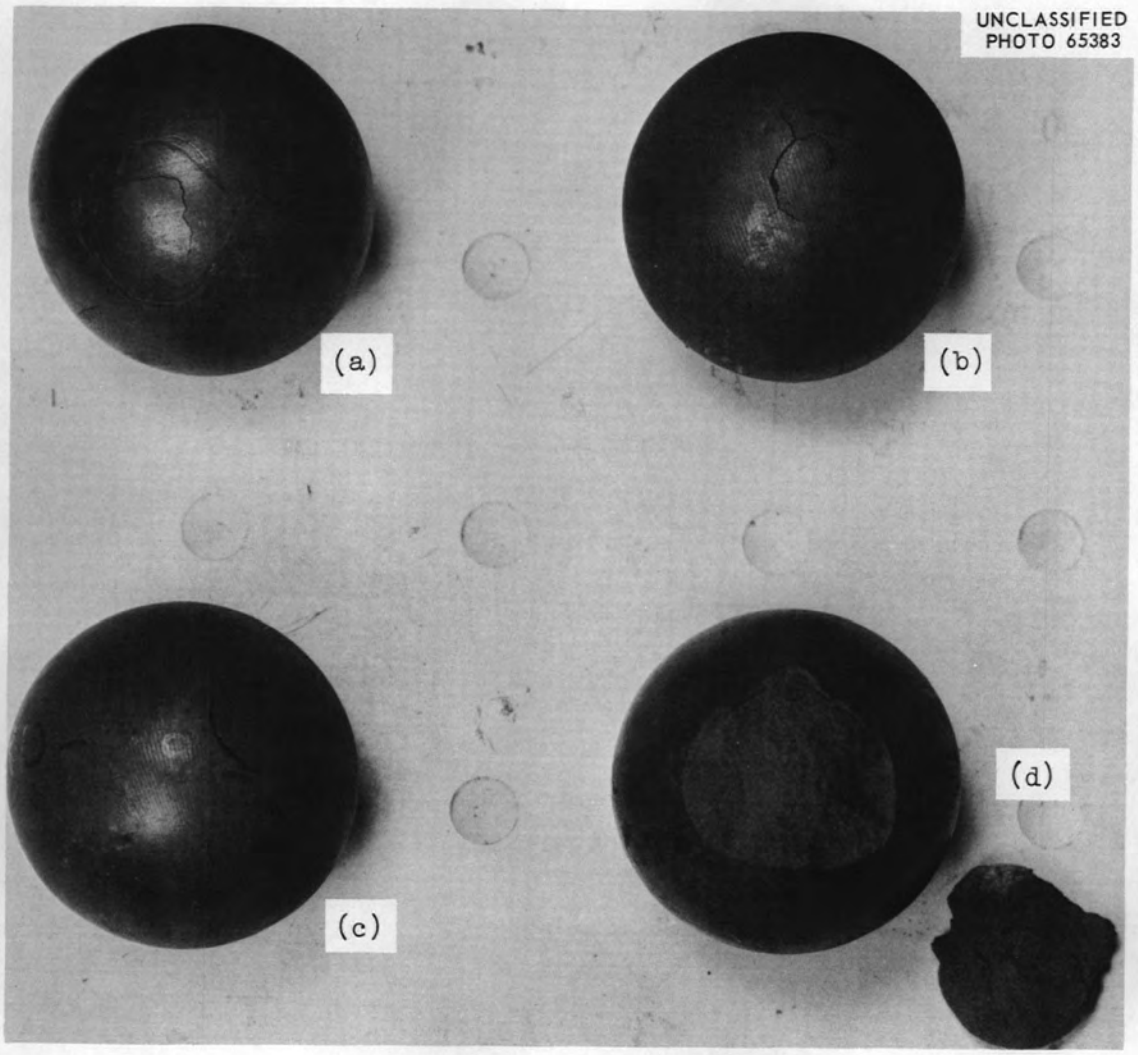

Fig. 9. Typical Failures in ATJ Graphite Spheres Dropped from 13 m onto a Steel Plate.

(c) a crack with a section about to chip off, to (d) a section completely chipped off from the sphere. Free-drop failures (13 m) of all the other graphites tested were similar although many of the spheres split into two approximately equal pieces rather than chipping. Some ATJ spheres in free drop from 27.3 m also failed by splitting in two pieces.

Drop-weight failures of all graphites tested were similar in appearance to the free-drop failures (Fig. 37, appendix). Spheres that were crushed normally failed by splitting into two or three pieces with some of them having an additional "conical" piece where the steel plates bore on the spheres (Fig. 38, appendix).

Typical free-drop failures of other grades of graphite are shown in Figs. 39 and 40 in the appendix.

Free-drop failures in ATJ suggested that all the damage occurred near the surface and might be cumulative. Several sets of 6-cm-diam spheres from the same lot of ATJ graphite were dropped varying numbers of times from 5 m onto a steel plate, and those that had not failed were crushed. The results are shown in Fig. 10; the crushing strength does decrease with the number of drops, indicating some damage does accumulate. The relatively small decrease, however, suggests that this is a "surface" effect.

Fifteen spheres (6-cm diam) of ATJ were dropped from 5 m onto a steel plate until failure or 190 drops, whichever was less. Seven spheres failed before 190, one failed on drop 190, and the other seven had not failed at 190 (Fig. 41, appendix). A photomicrograph of the one that failed at drop 190 is shown in Fig. 11. This section and other sections at higher magnification suggest that repeated impact of solid spheres may break the graphite between the normal voids to give fissures, which are roughly parallel to the sphere surface. Smaller spheres (1.5-in. diam) were machined concentrically from the remaining 14 spheres and were crushed. There was no correlation between crushing strength and the number of drops to failure; nor was there any difference in crushing strength between those that had failed by dropping and those that had not.

One sphere which was dropped on the steel plate from 27.3 m was sectioned and metallographically examined. There was no detectable difference in appearance (at 100×) between the region of the sphere that impacted on the plate and virgin graphite from the same lot (Fig. 42, appendix).

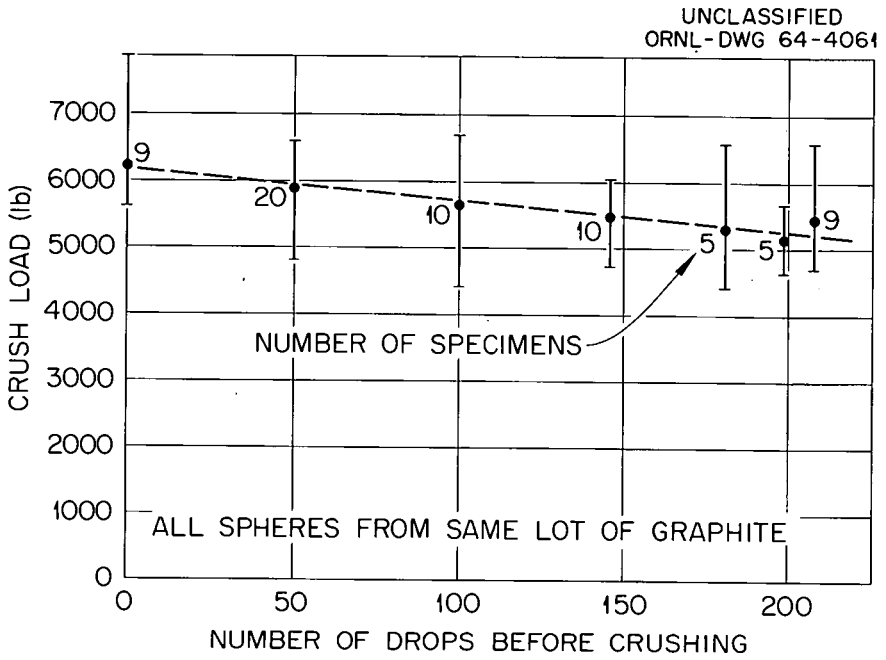

Fig. 10. Crushing Load of 6-cm-diam Spheres of ATJ Graphite (Unfailed) After Dropping from 5 m with Random Orientation onto Steel Plate.

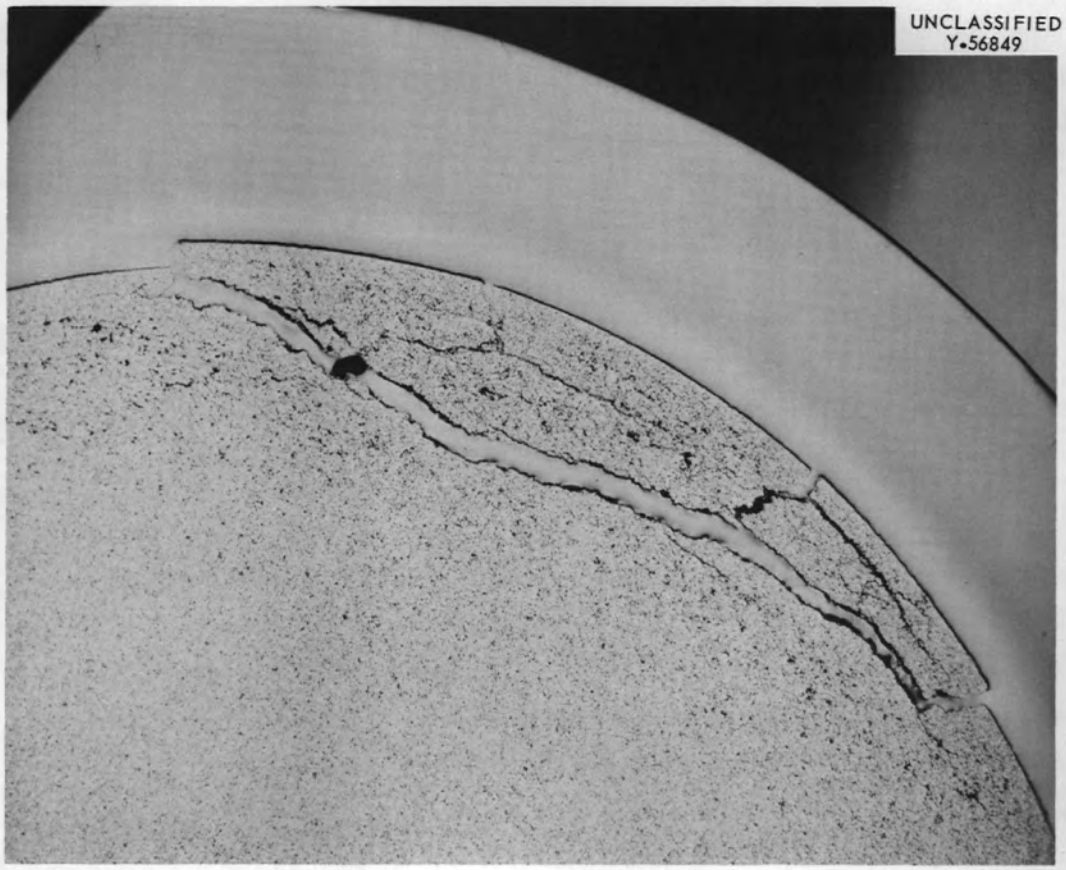

Fig. 11. Section of 6-cm-diam ATJ Graphite Sphere that Failed on Drop 190 from 5 m onto a Steel Plate. As polished. 3×.

Smaller spheres (1.5-in. diam) were also machined concentrically from 6-cm-diam spheres that had been tested to failure in 13-m-free-drop and in drop-weight tests. Three spheres from each set (poorest, best, and closest to the average) were radiographed before all were crushed. The radiographs showed nothing in these 1.5-in.-diam spheres that we could interpret as a flaw. The results of crushing tests of those spheres that had failed in drop-weight tests are shown in Fig. 12. Data from free-drop tests were similar (Figs. 43 and 44, appendix). These clearly indicate that all damage took place in an outer annular region which is not more than 7/16 in. thick.

IMPACT RESISTANCE OF FUEL ELEMENTS

Since ATJ, in solid spheres, proved superior to the other seven grades tested, essentially all tests of the machined-shell concept of AVR fuel elements used ATJ for the shell material.

Specimens and Test Methods

All AVR fuel elements assembled and tested at ORNL consisted of a machined socket, a machined plug, and a machined sphere of CS-312 graphite to simulate the molded fueled insert of an actual fuel element. In all cases, the three pieces were cemented together with carbon cement and then baked in flowing hydrogen to coke the cement. The bakeout cycle was cam controlled to increase from room temperature to 400°C in 22 hr (essentially linear), from 400 to 1000°C in 13 hr, followed by holding at 1000°C for 45 min. Power was shut off and the elements allowed to cool to room temperature in the furnace. Total cycle time was approximately 48 hr.

Eight different shell models, shown schematically in Fig. 13, were used. Models A, H, and I were made with "lugs" so that torque could be applied and measured with the lug being machined to a spherical contour afterward. Models B, G, J, and K were machined directly to spherical contours so that no measurement of closure torque was possible. All models except G and the slip plug had threaded closures with variations in the number of threads per inch, in rounding of the thread at peak and root, and in

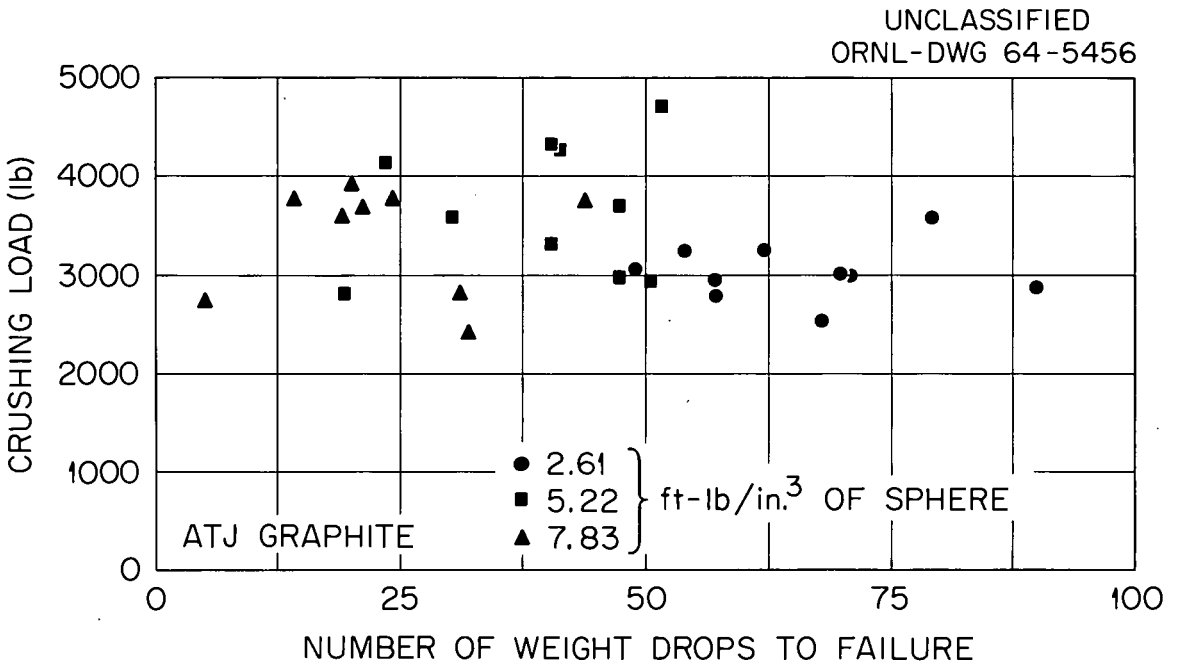

Fig. 12. Crushing Load of 1 1/2-in.-diam Spheres Machined Concentrically from 6-cm-diam Spheres After Failure in Drop-Weight Tests.

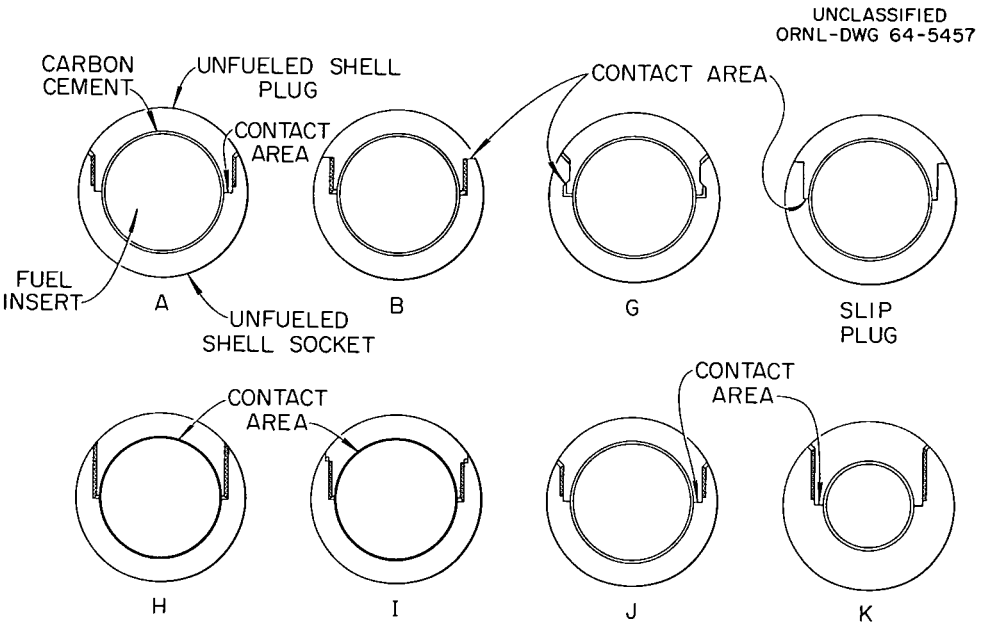

Fig. 13. Schematic AVR Fuel Element Design.

region of contact between socket, plug, and insert. Model G had a bayonet-type closure with four lugs. Although preliminary testing indicated the slip plug was probably superior to threaded closures, it was not investigated further. This action was taken because the cement bond might possibly rupture in reactor operation and allow the plug to come free, while breaking of the cement bond in a threaded closure would still leave the socket and plug intact although weakened. Figures 45 and 46 in the appendix show actual models.

Fuel elements were tested in free drop only. The elements were dropped from 4 m onto a three-deep bed of closely packed 6-cm-diam spheres of CS-312. Dropping continued to failure or to 75 drops (150% of the tentative specifications), whichever was less. All elements surviving 75 drops were then dropped from 4 m onto a steel plate until failure.

Effect of Design and Fabrication Variables

Preliminary testing indicated, as anticipated, that the thicker the shell the greater the number of drops required for failure. Thicker shells, however, imply higher central temperatures and greater thermal stresses, both of which are undesirable. A shell thickness of 0.8 cm (0.315 in.) was chosen as a reasonable compromise.

We anticipated that increasing closure torque might decrease impact resistance through increased tensile stress in the threaded section of both socket and plug. The data showed that torque between 15 and 50 in.-lb (lines 4 and 6, respectively, in Table 2) had essentially no effect on the number of drops. As a result, the lugs of model A were eliminated on most of the later models.

Sockets, plugs, and inserts, as machined, had some fine dust on the surface. Since similar dust is harmful in gluing wood, analogous behavior seemed possible with graphite. A number of elements were ultrasonically cleaned before assembly. When no real difference in behavior was found (e.g., lines 1 and 4 and lines 2 and 5, Table 2), cleaning was abandoned.

Three different carbon cements were tried. Comparison of lines 3 and 9 and lines 16 and 17, Table 2, indicates little difference. Most assembling was done with P-514 since it has a small-grained creamy texture while C-10 has some relatively large particles, which makes it more difficult to use in small spaces between shell and insert.

Table 2. Results of Free-Drop Tests of Simulated AVR Fuel Elements,[a] 6-cm-diam and 0.8-cm-thick-wall ATJ Graphite Shells, CS-312 Inserts

Line Number	Model Type	Nominal Radial Clearance (mils)	Cement Used	Portion Cemented	Ultrasonic Cleaning	Closure Torque (in.-lb)	Number of Specimens	Number of Drops for Failure from 4 m: Onto Bed of Spheres			Onto Steel Plate		
								Minimum	Average	Maximum	Minimum	Average	Maximum
1	A	5	P-514	All	Yes	15	5		75[b]		1	3.6	7
2	A	25	P-514	All	Yes	15	5	11	39.8	71			
3	A	40	P-514	All	Yes	15	10	8	23.0	41			
4	A	5	P-514	All	No	15	5		75[b]		1	4.2	10
5	A	25	P-514	All	No	15	5	31	39.0	48			
6	A	5	P-514	All	No	50	5		75[b]		3	6.8	15
7	A	5	P-514	Threads only	No	15	5	10	24.6	32			
8	A	40	P-514	Threads only	Yes	15	5	3	6.8	12			
9	A	40	C-10	All	Yes	15	5	22	29.6	52			
10	B	5	P-514	All	No	c	15	63	74.2[d]	75	1	1.9	5
11	B[e]	5	P-514	All	No	c	10	6	48.0[e,f]	75	1	3.2	7
12	G	5	P-514	All	Yes	g	4	39	47.5	58			
13	G	40	P-514	All	Yes	g	4	1	5.2	11			
14	H	40	P-514	All	No	15	5	75	75[f]	75	2	4.8	7
15	I	40	P-514	All	No	15	5	51	70.2[h]	75	1	1.7	3
16	J	25	P-514	All	No	c	10	18	47.5[h]	75	1	1.7	2
17	J	25	Hexalon	All	No	c	9	9	45.7[h]	75	1	1	1

[a]These data plus additional data are given in Table 4 in the appendix.
[b]All specimens survived without failure.
[c]Not measured.
[d]Fourteen specimens survived without failure.
[e]Grade AGOT graphite.
[f]Four specimens survived without failure.
[g]Torque not required.
[h]Three specimens survived without failure.

It is conceivable that the cement bond between shell and insert will break under reactor operating conditions. If this happens, the fuel element will sustain considerably fewer drops in the reactor, as shown by comparing elements having uncemented inserts with those having completely cemented inserts (lines 1 and 7 and lines 3 and 8 in Table 2).

Of all the variables considered, the nominal radial clearance between shell and insert is clearly the major factor in impact resistance of fuel elements. This is shown by lines 1, 2, and 3 in Table 2, by comparison of Fig. 14 (5 mil) and Fig. 15 (40 mil), and by Fig. 16. It is obvious that the smaller the radial clearance the greater the number of drops required for failure. Results for 25-mil clearance are shown in Fig. 47 in the appendix.

Figures 14 and 15 show that the small differences in design among models A, B, and J (all with threaded closures) are of no consequence. Model G, with its bayonet-type closure, which was suggested for possible improved ease in assembly, is clearly inferior to the other models. It was also more difficult to assemble.

It was anticipated that molded fueled inserts could not be controlled in manufacture to give a guaranteed clearance of less than approximately 25 mils. When models A and B indicated the large effect of radial clearance, model H was developed for use primarily with 25-mil or larger clearances. We hoped that screwing the plug into the socket until the socket, insert, and plug were in close contact would minimize the effect of a large clearance, despite the continued existence of this clearance around a circumference normal to the screw axis. The first few tests with model H (Fig. 15) were most attractive. Machining of the plug to a spherical contour, however, left a gap in the surface that exceeded the allowable. Model I, with a short unthreaded section but otherwise identical to model H, eliminated this surface gap but did not perform as well as the model H for no discernible reason. In addition, after the first few elements, difficulty was encountered as the first few threads of the plug broke off during assembly. When no ready solution of this problem was found, effort on these models was stopped with the hope of returning to them later. It should be noted that model H came from one lot of ATJ graphite while model I came from a different lot. Some of the model I's failed by chipping rather than

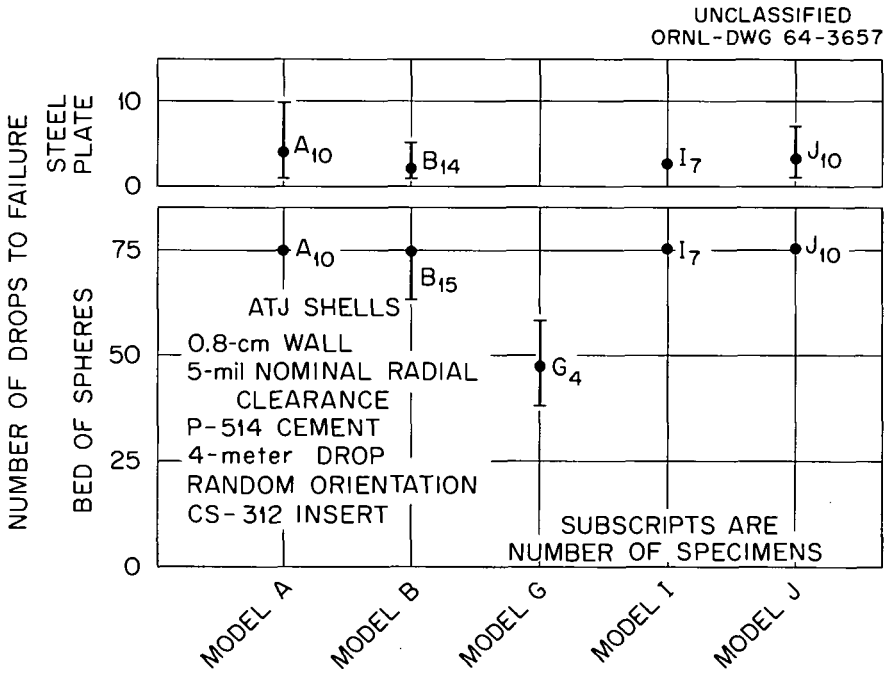

Fig. 14. Comparison of Number of Drops for Failure in Free-Drop Tests of Various Shell Models.

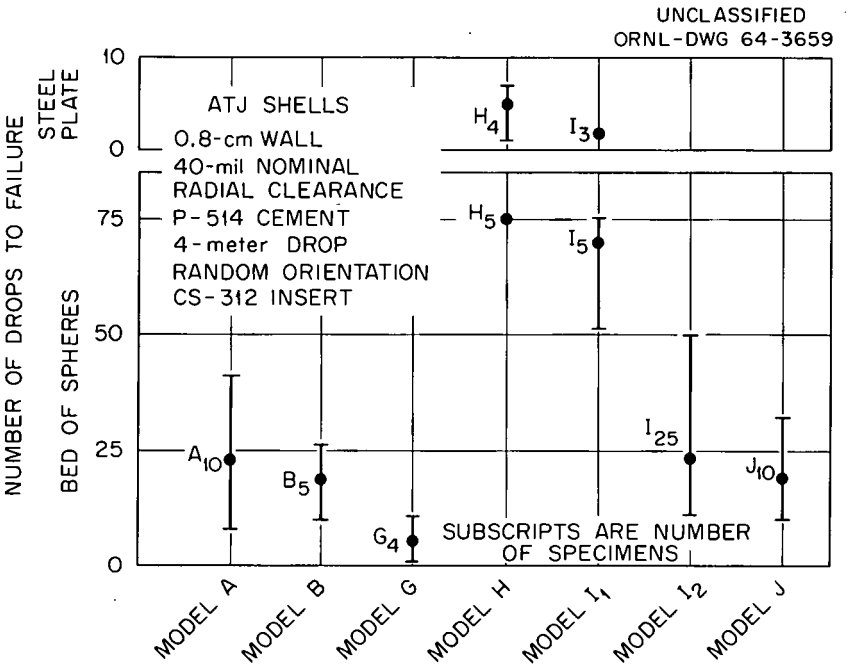

Fig. 15. Comparison of Number of Drops for Failure in Free-Drop Tests of Various Shell Models.

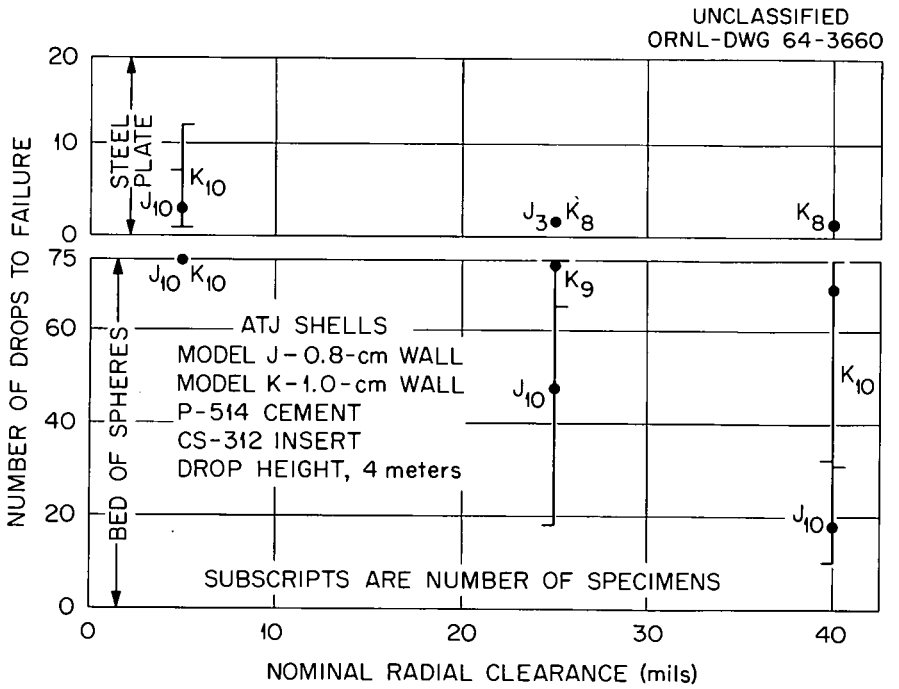

Fig. 16. Comparison of Number of Drops for Failure in Free-Drop Tests of Shell Models J and K.

cracking. Such chipping was not observed in any other models. We thus suspect an inferior block of graphite although we have no other evidence to support this suspicion.

Figure 16 shows the effect of changing shell thickness as well as the effect on radial clearance. The poorest model K element, with 1-cm-wall (0.394 in.) and 40-mil-radial clearance, was about as good as the best model J element with 0.8-cm-wall (0.315 in.) and the same radial clearance. Model K with 25-mil clearance exceeds the required 50 drops while model J does not, although this is based on rather limited data. The superiority of model K over model J with 5-mil clearance is not as obvious. No determination has been made of the relative effectiveness of a drop on the bed of spheres and on the steel plate, although obviously fewer drops are required for failure on the plate than on the bed of spheres. Orientation of the element is also much more critical when dropping on the plate since impact in the vicinity of the circumference normal to the screw axis may cause failure on the first drop, while impact in the direction of the axis may require many drops for failure.

Drop-weight tests of model K elements (kinetic energy of weight equivalent to element dropping 4 m) with 25-mil-radial clearance produced failure on the first drop on the circumference normal to the screw axis. In the direction of the screw axis, however, dropping on the cap required 22 drops and dropping on the socket required 23 drops for failure. A model K element with 5-mil-radial clearance failed on the first drop on the circumference normal to the screw axis, while a second model K element failed on drop 115 on the cap in the direction of the screw axis.

Thermal cycling in vacuum for 10 cycles between room temperature and 1000°C was performed on models J and K (10 elements per set, 25-mil-radial clearance). The number of drops for failure in both models was essentially the same for thermally cycled as for uncycled elements.

Essentially all of the elements tested had shells made from ATJ graphite. Two sets of elements using model B were made from AGOT. Lines 10 and 11, Table 2, using elements with 5-mil-radial clearance, show that AGOT is inferior to ATJ. With 40-mil clearance, there was little difference in the number of drops for failure. We suspect the effect of radial clearance obscures any effect of material difference.

Typical failures of elements are shown in Fig. 17. These range from (a) a small crack to (b) complete separation of socket, insert, and plug with further breaking of the threaded section. Represented by (c), most of the failures were cracks that extended various amounts around the circumference with other cracks running various amounts normal to the joint line between socket and plug. The two elements in (b) and (d) indicate that further work is needed on obtaining a more complete cement bond.

Other Concepts

In addition to the elements assembled at ORNL, we tested a few fueled, 6-cm-diam elements fabricated by other laboratories. The results of these tests are given in Table 3. The specimens were prepared essentially as follows:

1. GA-VS 15 — fueled insert which had been hot pressed and cemented, with "small" radial clearance, into a model A shell of ATJ supplied by ORNL,
2. GA-VS 16 — same as GA-VS 15 except that the insert was warm pressed and baked prior to cementing in the shell,
3. NCL-VS 2 — fueled insert injection molded into a machined ATJ shell having a wall thickness of 1 cm (0.394 in.); one of the specimens, after failure, is shown in Fig. 18,
4. 3M-VS 15 — fueled sphere, molded with no unfueled shell,
5. 3M-VS 17 — fueled sphere, molded with 1/8-in. unfueled shell,
6. 3M-VS 18 — fueled sphere, molded with 1/4-in. unfueled shell.

From the limited data in Table 3, it appears that GA-VS 15 and 16 have about the same impact resistance as the ORNL model A elements with 5-mil-radial clearance. The NCL-VS 2 specimens were designed so that the injection molded insert increases somewhat in size during the baking step to eliminate any radial clearance. Despite this, the specimens tested (with 1-cm-thick wall) had about the same impact resistance as the ORNL elements with 0.8-cm-thick wall and 5-mil-radial clearance. The all-molded 3M specimens are clearly the most impact resistant of any of the fuel element configurations tested with the specimens having a 1/4-in.-unfueled shell sustaining about as many drops from 4 m on the steel plate as solid ATJ spheres on dropping from 5 m. Thermal cycling in vacuum obviously decreases the impact resistance of the 3M specimens with unfueled shells. Typical failures are shown in Figs. 48 and 49 in the appendix.

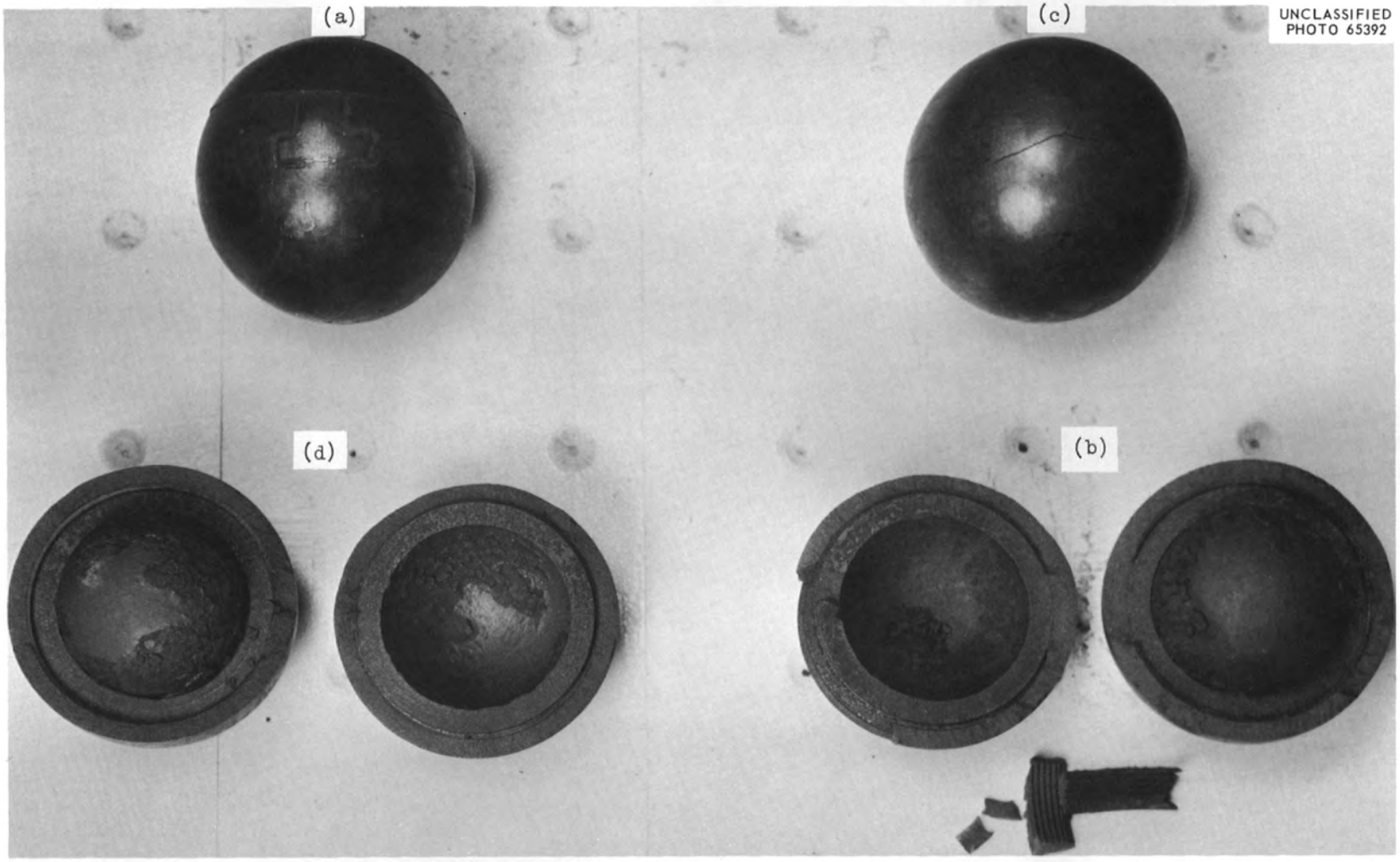

Fig. 17. Typical Failures in AVR Fuel Elements; 4-m Drop onto Bed of Graphite Spheres.

Table 3. Results of Free-Drop Tests on Fueled-Graphite Spheres from Other Laboratories

Specimen Number	Thermal Cycled	Number of Specimens	Number of Drops from 4 m			
			Bed of Spheres	Steel Plate		
				Minimum	Average	Maximum
GA-VS 15	No	2	75	1	1	1
GA-VS 16	No	2	75	1	1	1
NCL-VS 2	No	2	75	1	3	5
NCL-VS 2	Yes	2	75	1	2	3
3M-VS 15	No	3	75	76	95	114
3M-VS 15	Yes	3	75	75	90	105
3M-VS 17	No	2	75	109	163	217
3M-VS 18	No	3	75	254	266	279
3M-VS 18	Yes	2[a]	75	111	176	240

[a]A third specimen failed on the 16th drop onto the steel plate. The mode of failure strongly suggested poor bonding between core and shell.

Fig. 18. Grade NCL Fueled Sphere with 1-cm-thick ATJ Graphite and Injection Molded Insert. Free-drop test from 4 m.

CONCLUSIONS

The results of testing of solid spheres of graphite show:

1. Of the eight grades tested, impact resistance of molded graphites is better than that of extruded graphites with ATJ graphite the best.

2. Impact resistance of ATJ decreases as drop height increases although several drops are required for failure even on dropping 6-cm-diam spheres from 90 ft onto a steel plate.

3. Measured impact resistance depends on sphere size with best resistance in the smallest specimens.

4. Impact resistance varies from one block of ATJ to another with no correlation between impact resistance of a given sphere and the position within the block from which it came.

5. Bulk-density variations between 1.65 and 1.80 g/cm^3 have no effect on the impact resistance of ATJ.

6. All damage in ATJ from free-drop (13 m) and drop-weight tests occurs within the outer 7/16 in. of 6-cm-diam spheres.

7. Thermal cycling in vacuum can have an adverse effect on impact resistance of ATJ, while similar cycling in helium or hydrogen does not.

Free-drop tests of simulated AVR fuel elements using solid CS-312 graphite spheres as inserts in machined ATJ shells show:

1. Dropping an element from a given height onto a steel plate is far more drastic treatment than dropping onto a bed of graphite spheres. Relatively small differences in elements cannot be detected by dropping on the plate.

2. Essentially all elements fail in the vicinity of the circumference normal to the screw axis of the socket and plug.

3. ATJ is superior to AGOT for shell material as predicted by tests of solid spheres.

4. Small differences in design of elements having threaded closures (e.g., number of threads per inch) have no effect on impact resistance.

5. Variations in plug-closure torques between 15 and 50 in.-lb. have no effect on impact resistance.

6. There is no real difference in impact resistance among the three cements used.

7. Preassembly ultrasonic cleaning has no effect on impact resistance.

8. Elements with completely cemented inserts are clearly superior to elements with uncemented inserts.

9. Thermal cycling in vacuum has no effect on impact resistance.

10. The nominal radial clearance between insert and shell is a major factor in determining impact resistance. Shells with 0.8-cm-thick walls are satisfactory for clearances of 0.005 to 0.010 in., but 1.0- to 1.2-cm-thick shells would be required for clearances of 0.020 to 0.025 in.

11. Limited data indicate that all-molded elements are superior to machined-shell elements, although they lose some impact resistance upon thermal cycling in vacuum.

RECOMMENDATIONS FOR FUTURE INVESTIGATIONS

A number of aspects of this investigation merit consideration if additional work is conducted in the future. Among these are:

1. the effect of thermal cycling in vacuum on ATJ (and other) graphite,
2. socket and plug design, with particular reference to models H and I,
3. carbon cement with respect both to variety of cement and the bond formed between insert and shell,
4. nominal radial clearance between insert and shell with better definition of the relationship between clearance and shell thickness required.

APPENDIX

Page

Fig. 19. Comparison of Number of Drops for Failure in Drop-Weight Tests. 41

Fig. 20. Comparison of Load Required to Crush Eight Grades of Graphite. 41

Fig. 21. Relationship Between Drop-Weight Resistance and Crushing Strength of Seven Graphites; 1 1/2-in.-diam Solid Spheres. 42

Fig. 22. Relationship Between Free-Drop and Drop-Weight Resistances of Seven Graphites; 1 1/2-in.-diam Solid Spheres. 42

Fig. 23. Effect of Kinetic Energy on Failure of 6-cm-diam ATJ Graphite Spheres in Drop-Weight Tests. 43

Fig. 24. Effect of Kinetic Energy of Weight on Failure of 1 1/2-in.-diam ATJ Graphite Spheres in Drop-Weight Tests; 2.93-lb Weight. 44

Fig. 25. Effect of Momentum of Weight on Failure of 6-cm-diam ATJ Graphite Spheres in Drop-Weight Tests; 12.13-lb Weight. . 45

Fig. 26. Effect of Momentum of Weight on Failure of 1 1/2-in.-diam ATJ Graphite Spheres in Drop-Weight Tests; 2.93-lb Weight. 46

Fig. 27. Comparison of ATJ Graphite Specimens Used for Size-Effect Studies. 47

Fig. 28. Effect of Sphere Size on Number of Drops for Failure in Drop-Weight Tests of ATJ Graphite Spheres. 48

Fig. 29. Effect of Sphere Size on Nominal Crushing Stress of ATJ Graphite Spheres. 49

Fig. 30. Effect of Maximum Force on Failure of 1 1/2-in.-diam ATJ Graphite Spheres in Drop-Weight Tests; 2.93-lb Weight. . 50

Fig. 31. Variation in Failure in Drop-Weight Tests; Nine Lots of ATJ Graphite; 6-cm-diam Solid Sphere. 51

Fig. 32. Variation in Crushing Strength; 11 Lots of ATJ Graphite; 6-cm-diam Solid Spheres. 51

Fig. 33. Relationship Between Density and Drops for Failure in Drop-Weight Tests of 6-cm-diam Solid ATJ Graphite Spheres; 2.61 ft-lb/in.^{3} of Sphere. 52

Fig. 34. Relationship Between Density and Crushing Load of 6-cm-diam Solid ATJ Graphite Spheres. 52

Page

Fig. 35. Effect of 10 Thermal Cycles from Room Temperature to 1000°C on Failure in Free-Drop Tests of 6-cm-diam ATJ Graphite Spheres; Drop with Random Orientation onto Steel Plate from 13 m. 53

Fig. 36. Effect of 10 Thermal Cycles from Room Temperature to 1000°C on Crushing Load of 6-cm-diam ATJ Graphite Spheres. 53

Fig. 37. Typical Failures in 6-cm-diam ATJ Graphite Spheres in Drop-Weight Tests with 18.07 ft-lb of Kinetic Energy in Weight. 54

Fig. 38. Typical Failures in 6-cm-diam ATJ Graphite Spheres in Crushing Tests. 55

Fig. 39. Typical Failures in 6-cm-diam Graphite Spheres Dropped from 13 m onto a Steel Plate. Left: Grade 9050. Right: Grade HLM-85. 56

Fig. 40. Typical Failures in 6-cm-diam Graphite Spheres Dropped from 13 m onto a Steel Plate. Left: Grade CS-312. Right: Grade AGOT. 57

Fig. 41. Crushing Load of 1 1/2-in.-diam Spheres of ATJ Graph Graphite Machined Concentrically from 6-cm-diam Spheres After Dropping from 5 m with Random Orientation onto Steel Plate. 58

Fig. 42. Microstructure of ATJ Graphite. (a) Region of impact after dropping onto steel plate from 27.3 m. As polished. (b) Region diametrically opposite impact region in (a) above. As polished. 59

Fig. 43. Crushing Load of 1 1/2-in.-diam Spheres Machined Concentrically from 6-cm-diam Spheres After Failure in Free-Drop Tests from 13 m with Random Orientation onto Steel Plate. 60

Fig. 44. Crushing Strength of 1 1/2-in.-diam Spheres Machined from Virgin Stock or Concentrically from 6-cm-diam Spheres After Free Drop on Steel Plate or Drop-Weight Tests; ATJ Graphite. 60

Fig. 45. Four Shell Models Before Assembly. 61

Fig. 46. Four Shell Models Before Assembly. 62

Fig. 47. Comparison of Number of Drops for Failure in Free-Drop Tests of Various Shell Models. 63

Fig. 48. Failures in All-Molded Fueled Spheres (3M) in Free-Drop Tests. 64

Fig. 49. Failures in All-Molded Fueled Spheres (3M) After Thermal Cycling in Free-Drop Test. 65

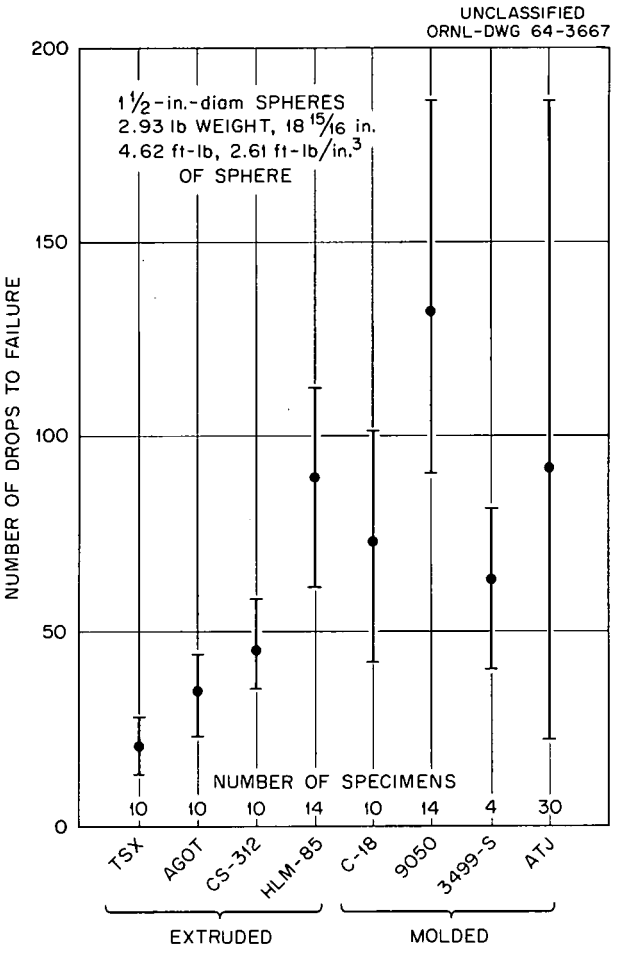

Fig. 19. Comparison of Number of Drops for Failure in Drop-Weight Tests.

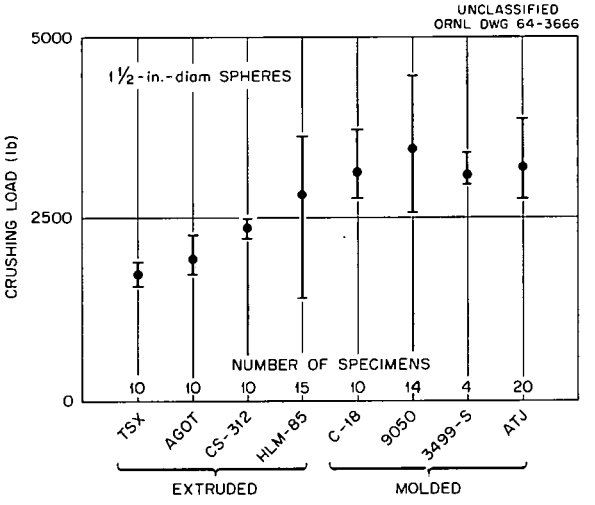

Fig. 20. Comparison of Load Required to Crush Eight Grades of Graphite.

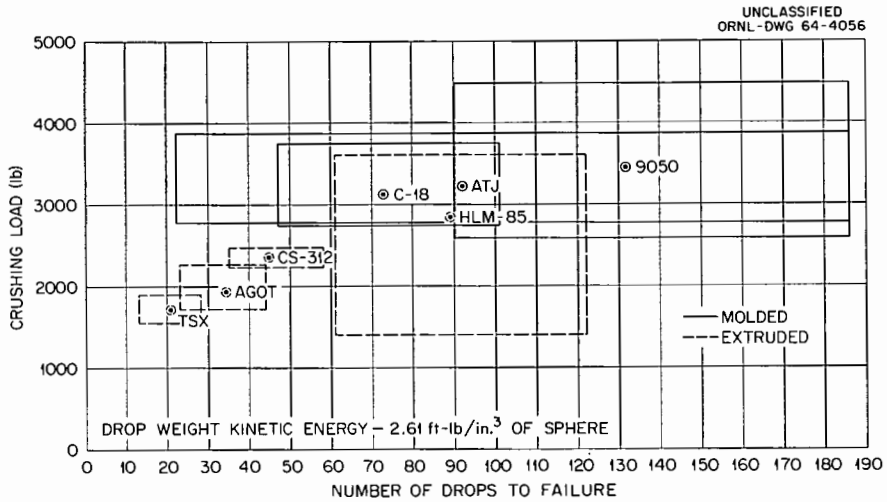

Fig. 21. Relationship Between Drop-Weight Resistance and Crushing Strength of Seven Graphites; 1 1/2-in.-diam Solid Spheres.

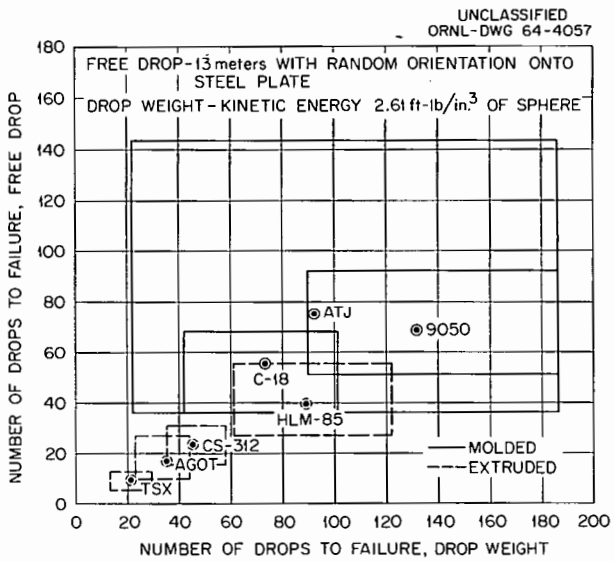

Fig. 22. Relationship Between Free-Drop and Drop-Weight Resistance of Seven Graphites; 1 1/2-in.-diam Solid Spheres.

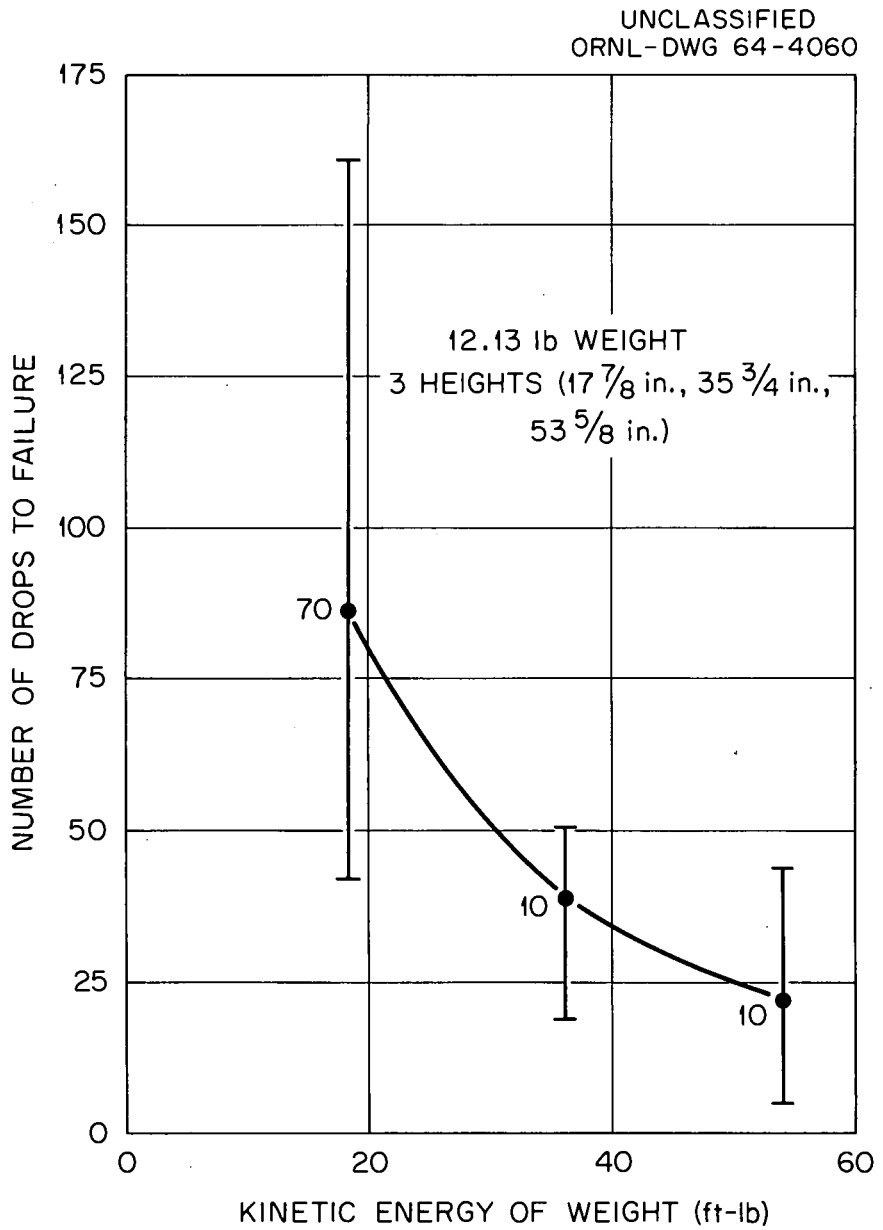

Fig. 23. Effect of Kinetic Energy on Failure of 6-cm-diam ATJ Graphite Spheres in Drop-Weight Tests.

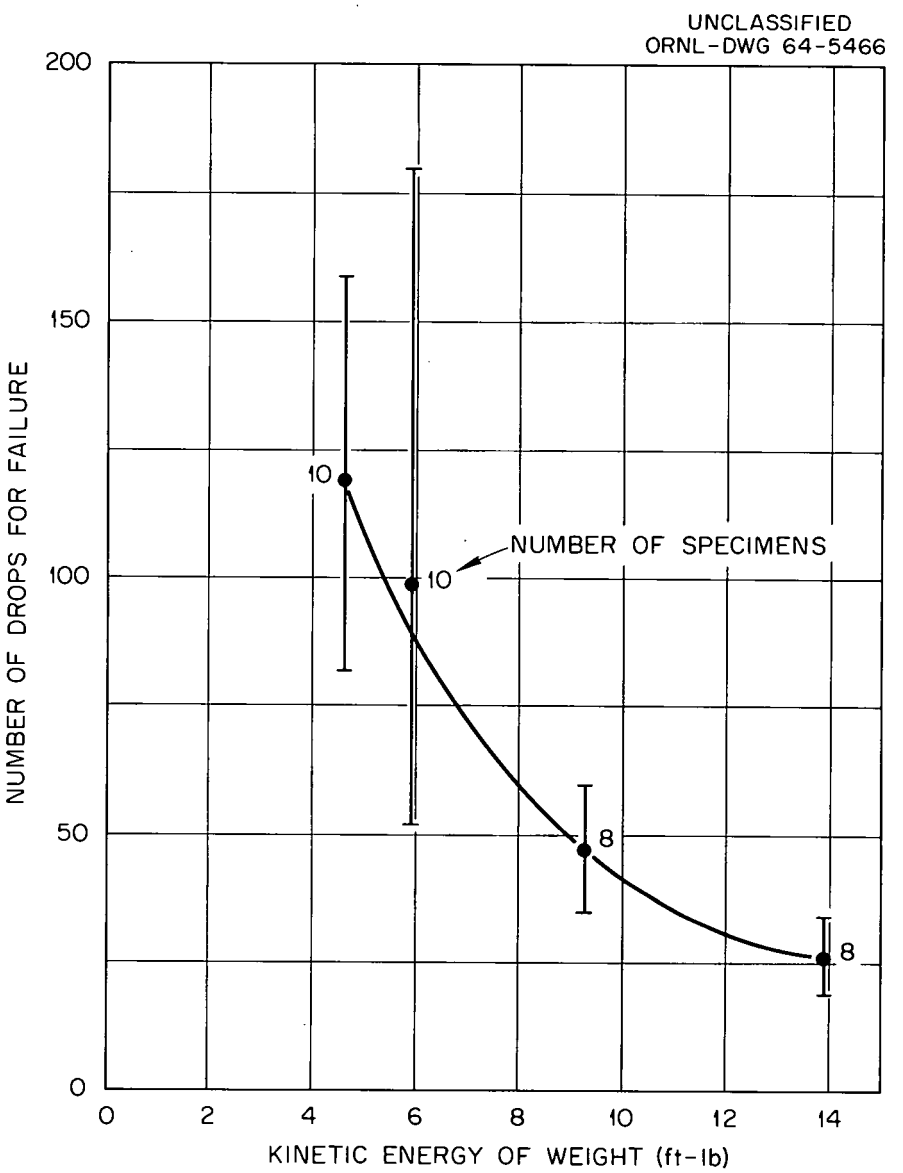

Fig. 24. Effect of Kinetic Energy of Weight on Failure of 1 1/2-in.-diam ATJ Graphite Spheres in Drop-Weight Tests; 2.93-lb Weight.

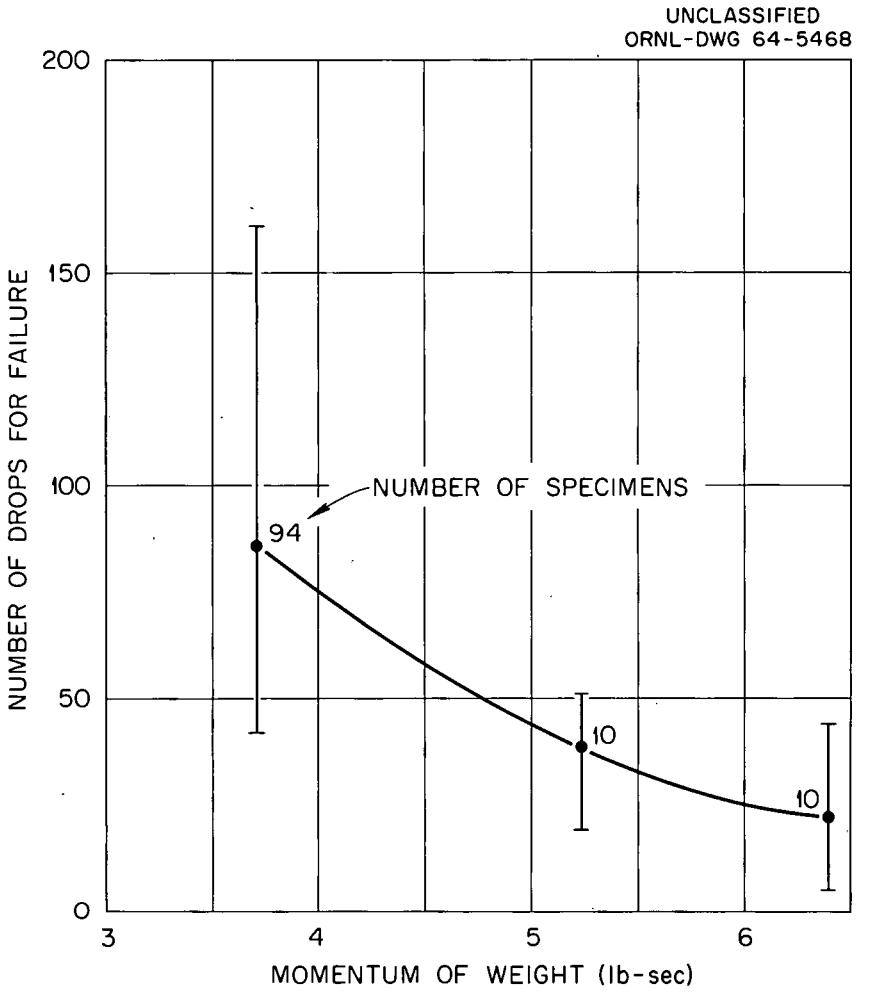

Fig. 25. Effect of Momentum of Weight on Failure of 6-cm-diam ATJ Graphite Spheres in Drop-Weight Tests; 12.13-lb Weight.

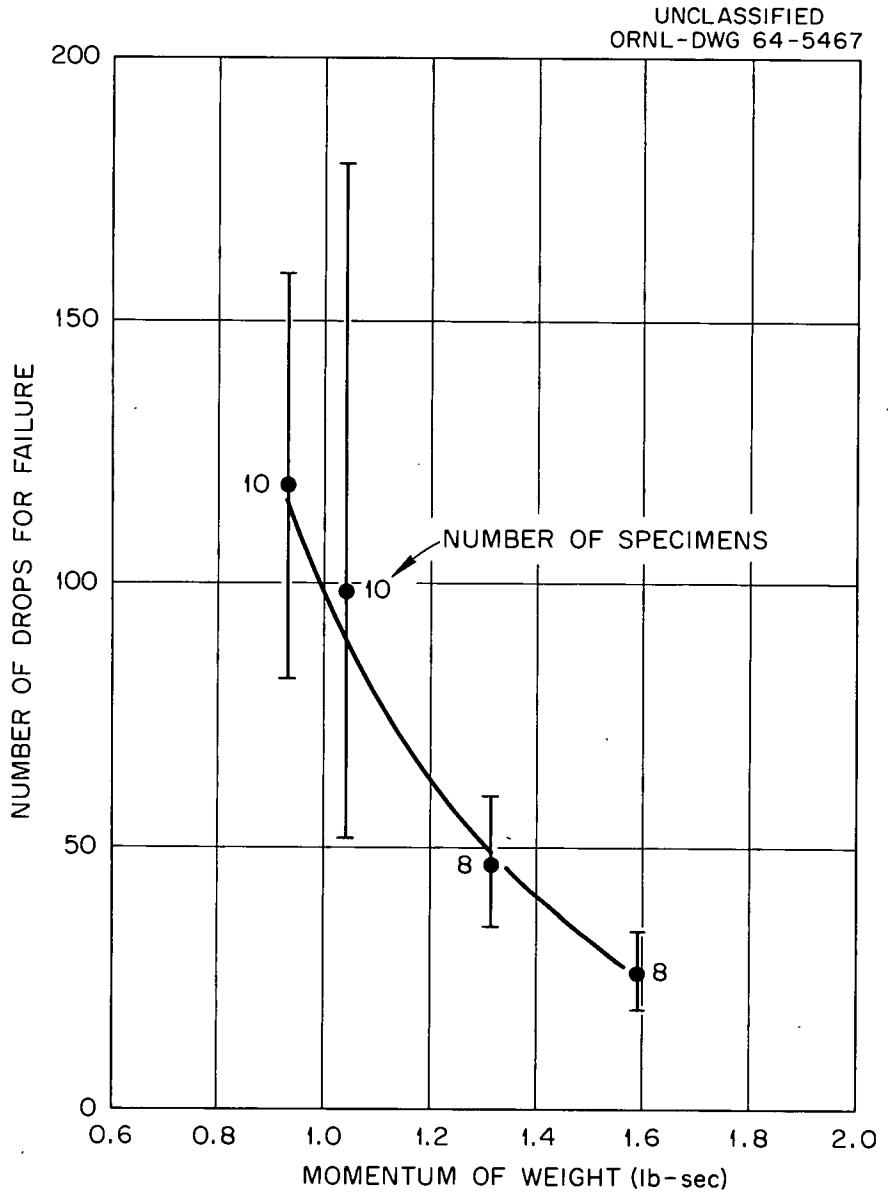

Fig. 26. Effect of Momentum of Weight on Failure of 1 1/2-in.-diam ATJ Graphite Spheres in Drop-Weight Tests; 2.93-lb Weight.

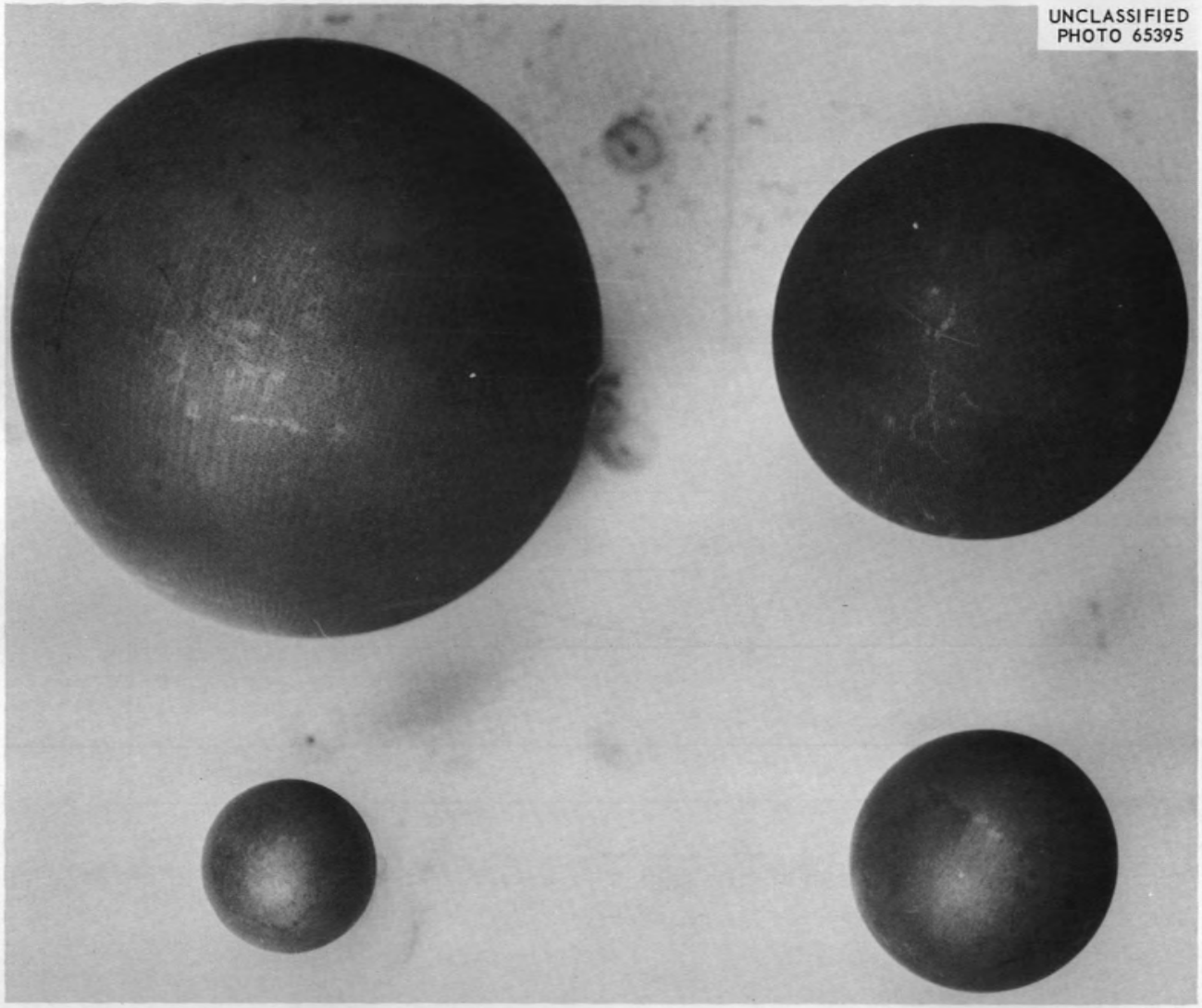

Fig. 27. Comparison of ATJ Graphite Specimens Used for Size-Effect Studies.

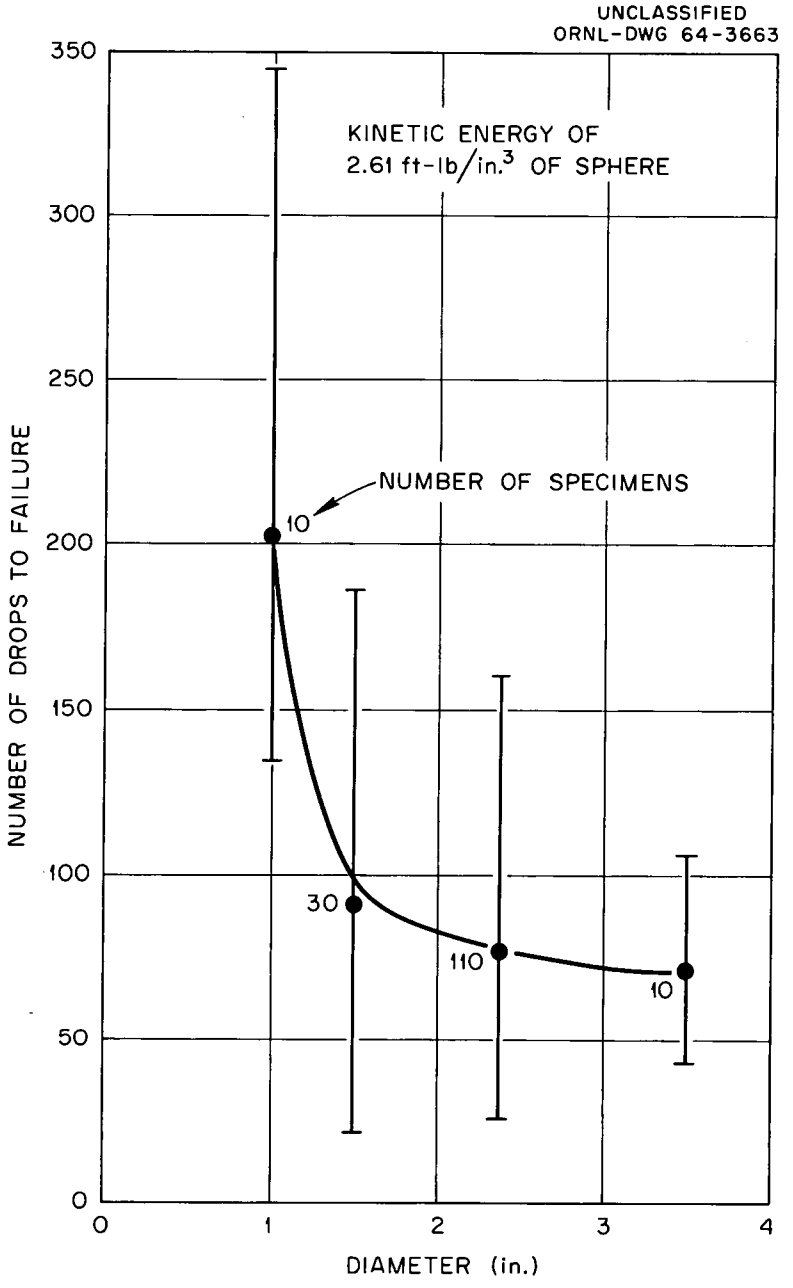

Fig. 28. Effect of Sphere Size on Number of Drops for Failure in Drop-Weight Tests of ATJ Graphite Spheres.

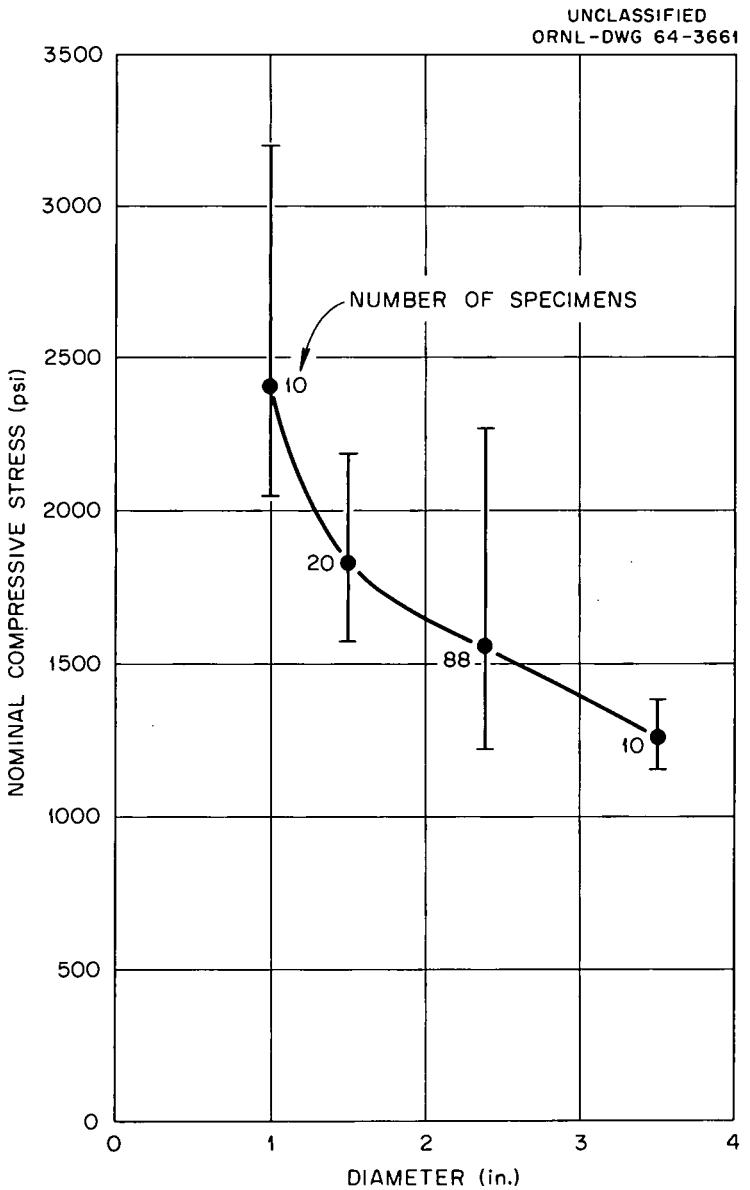

Fig. 29. Effect of Sphere Size on Nominal Crushing Stress of ATJ Graphite Spheres.

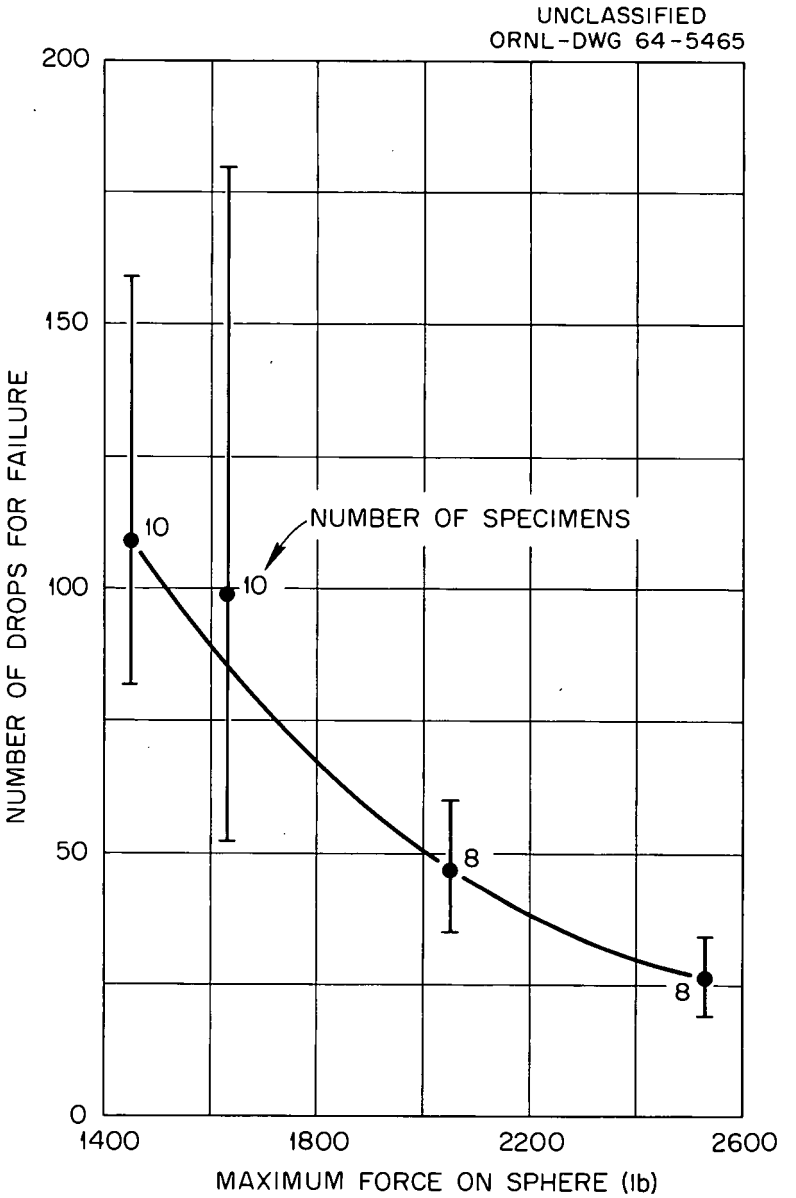

Fig. 30. Effect of Maximum Force on Failure of 1 1/2-in.-diam ATJ Graphite Spheres in Drop-Weight Tests; 2.93-lb Weight.

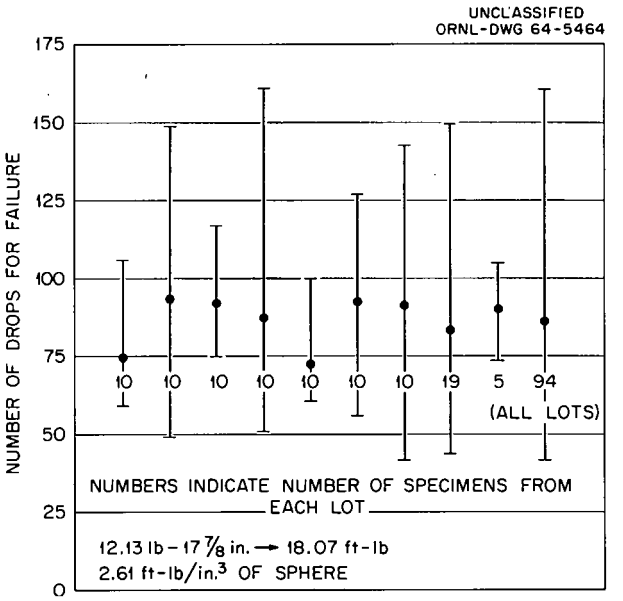

Fig. 31. Variation in Failure in Drop-Weight Tests; Nine Lots of ATJ Graphite; 6-cm-diam Solid Sphere.

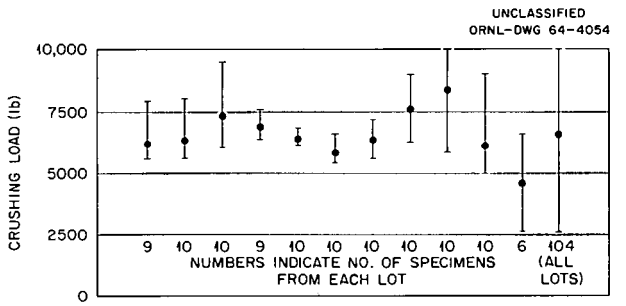

Fig. 32. Variation in Crushing Strength; 11 Lots of ATJ Graphite; 6-cm-diam Solid Spheres

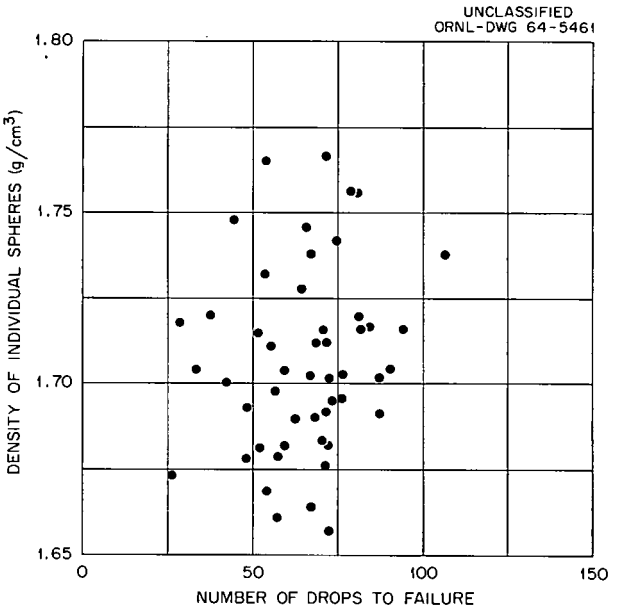

Fig. 33. Relationship Between Density and Drops for Failure in Drop-Weight Tests of 6-cm-diam Solid ATJ Graphite Spheres; 2.61 ft-lb/in.^{3} of Sphere.

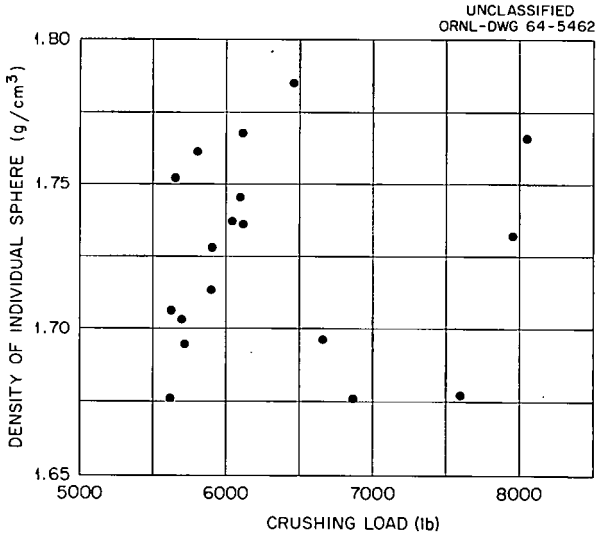

Fig. 34. Relationship Between Density and Crushing Load of 6-cm-diam Solid ATJ Graphite Spheres.

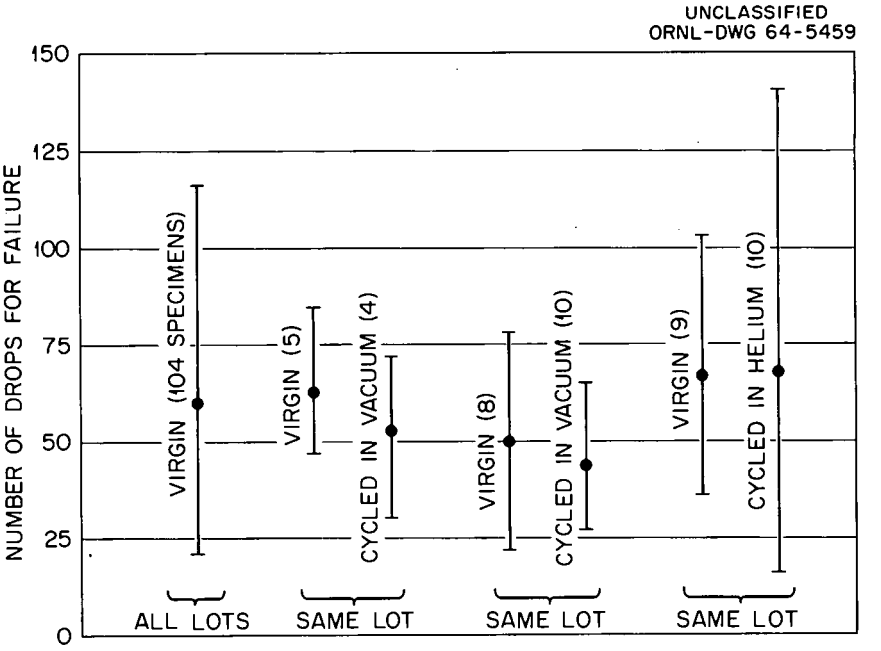

Fig. 35. Effect of 10 Thermal Cycles from Room Temperature to 1000°C on Failure in Free-Drop Tests of 6-cm-diam ATJ Graphite Spheres; Drop with Random Orientation onto Steel Plate from 13 m.

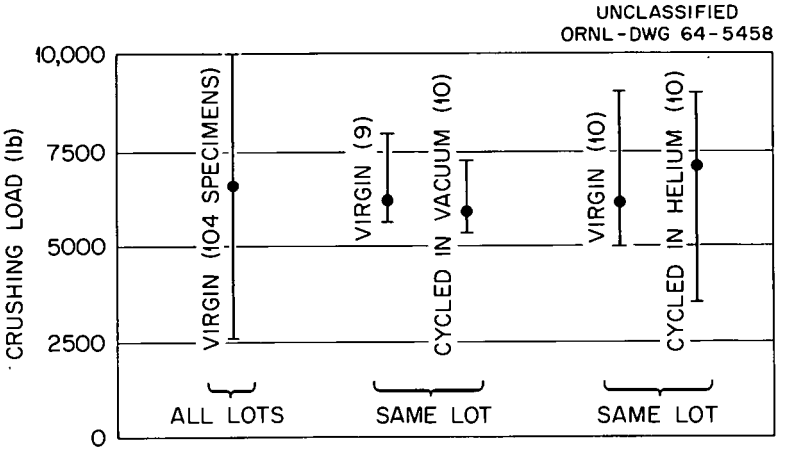

Fig. 36. Effect of 10 Thermal Cycles from Room Temperature to 1000°C on Crushing Load of 6-cm-diam ATJ Graphite Spheres.

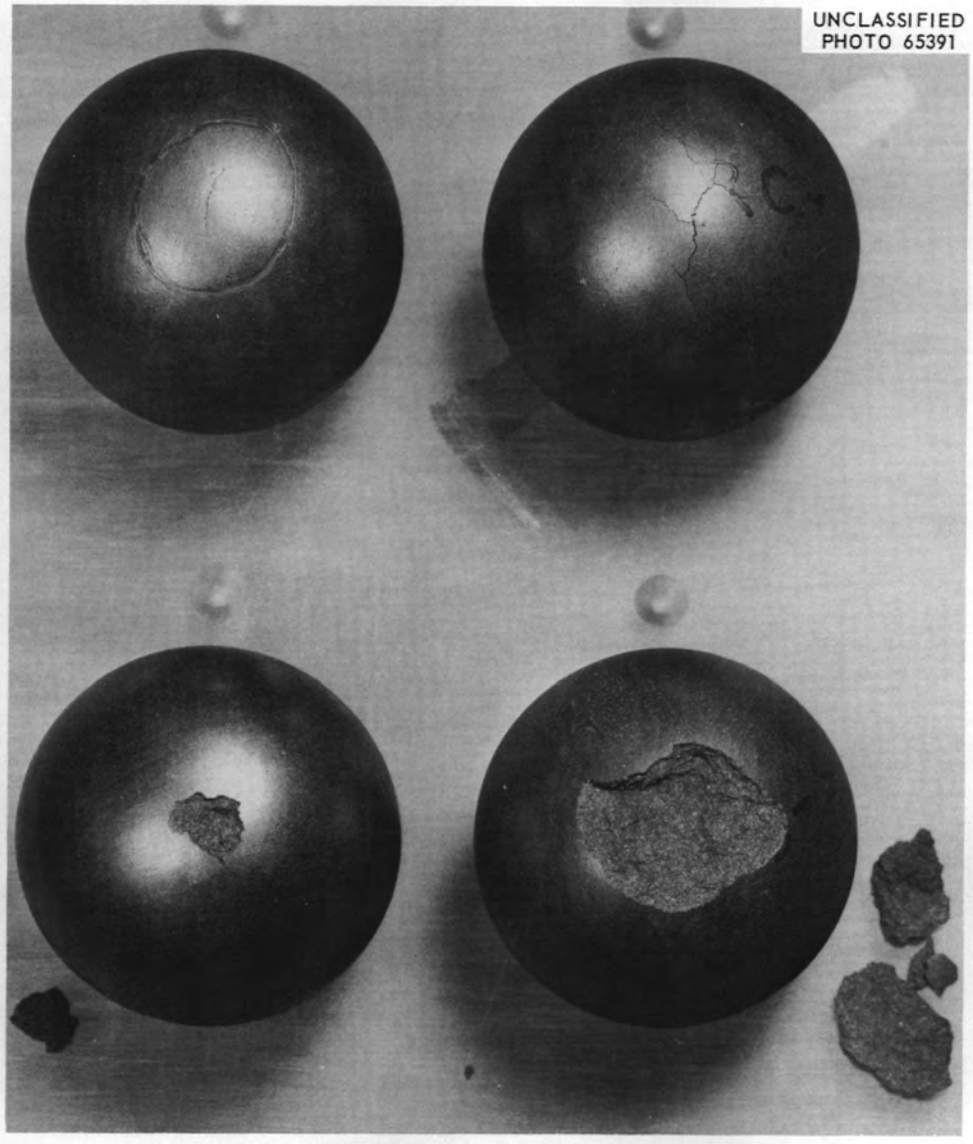

Fig. 37. Typical Failures in 6-cm-diam ATJ Graphite Spheres in Drop-Weight Tests with 18.07 ft-lb of Kinetic Energy in Weight.

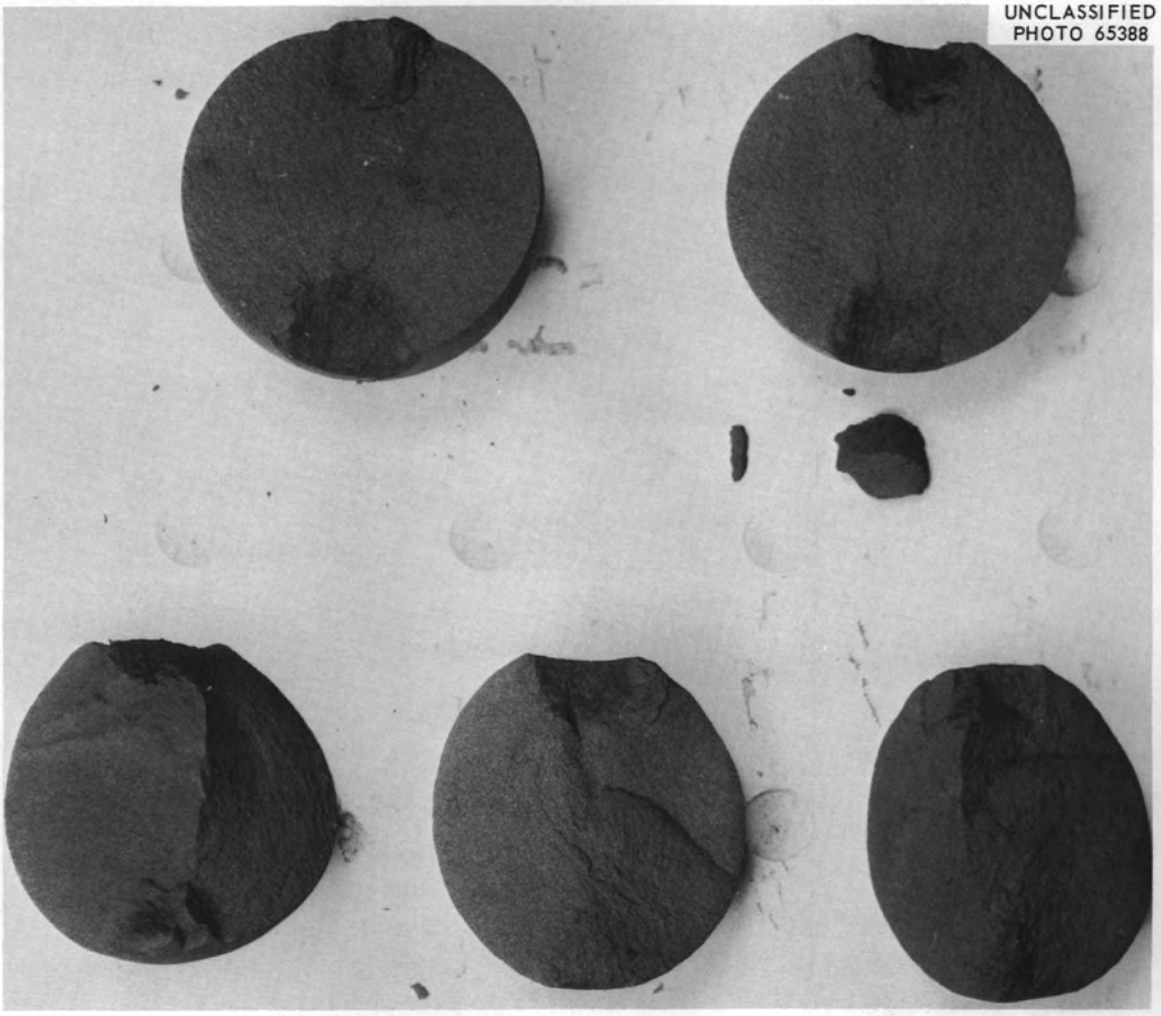

Fig. 38. Typical Failures in 6-cm-diam ATJ Graphite Spheres in Crushing Tests.

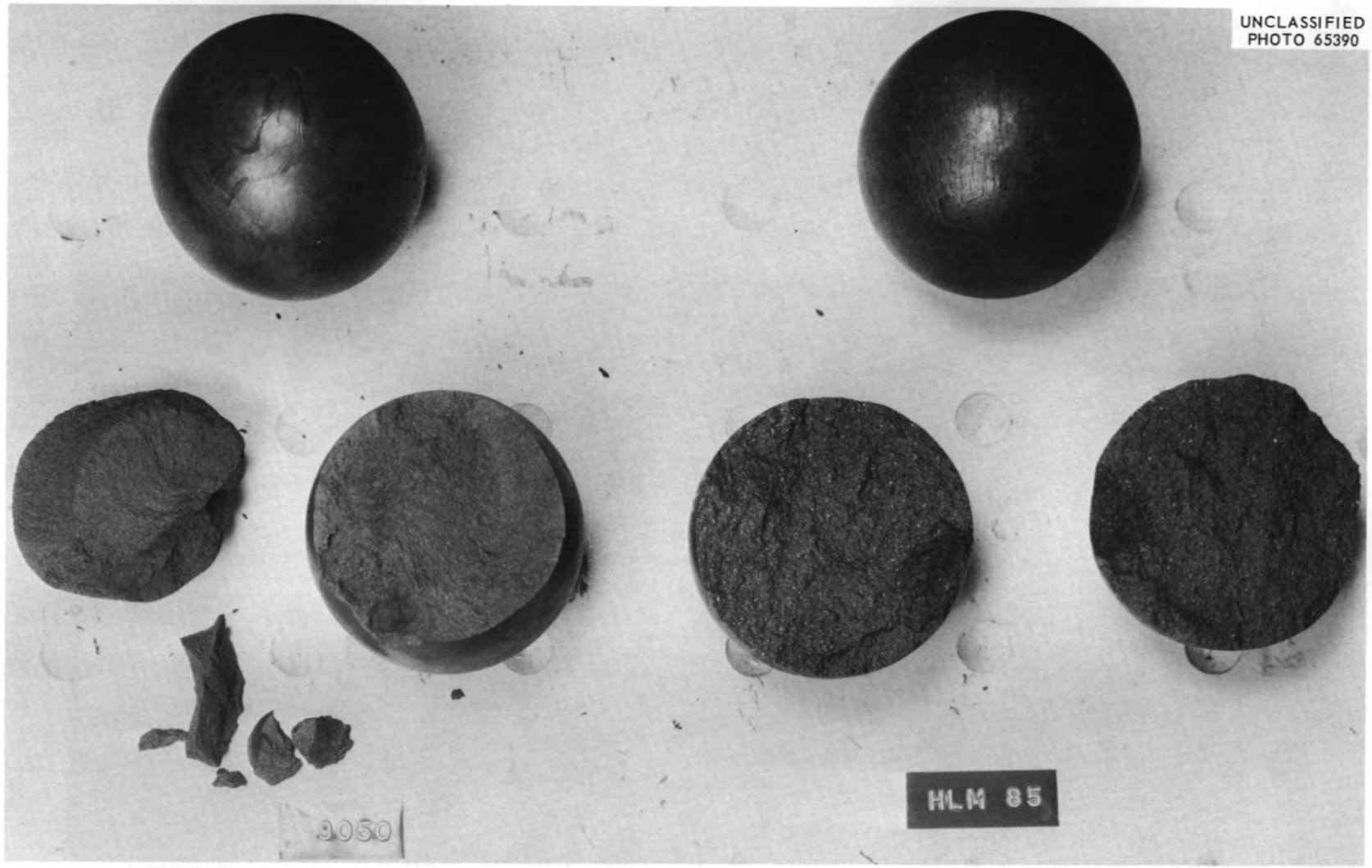

Fig. 39. Typical Failures in 6-cm-diam Graphite Spheres Dropped from 13 m onto a Steel Plate. Left: Grade 9050. Right: Grade HLM-85.

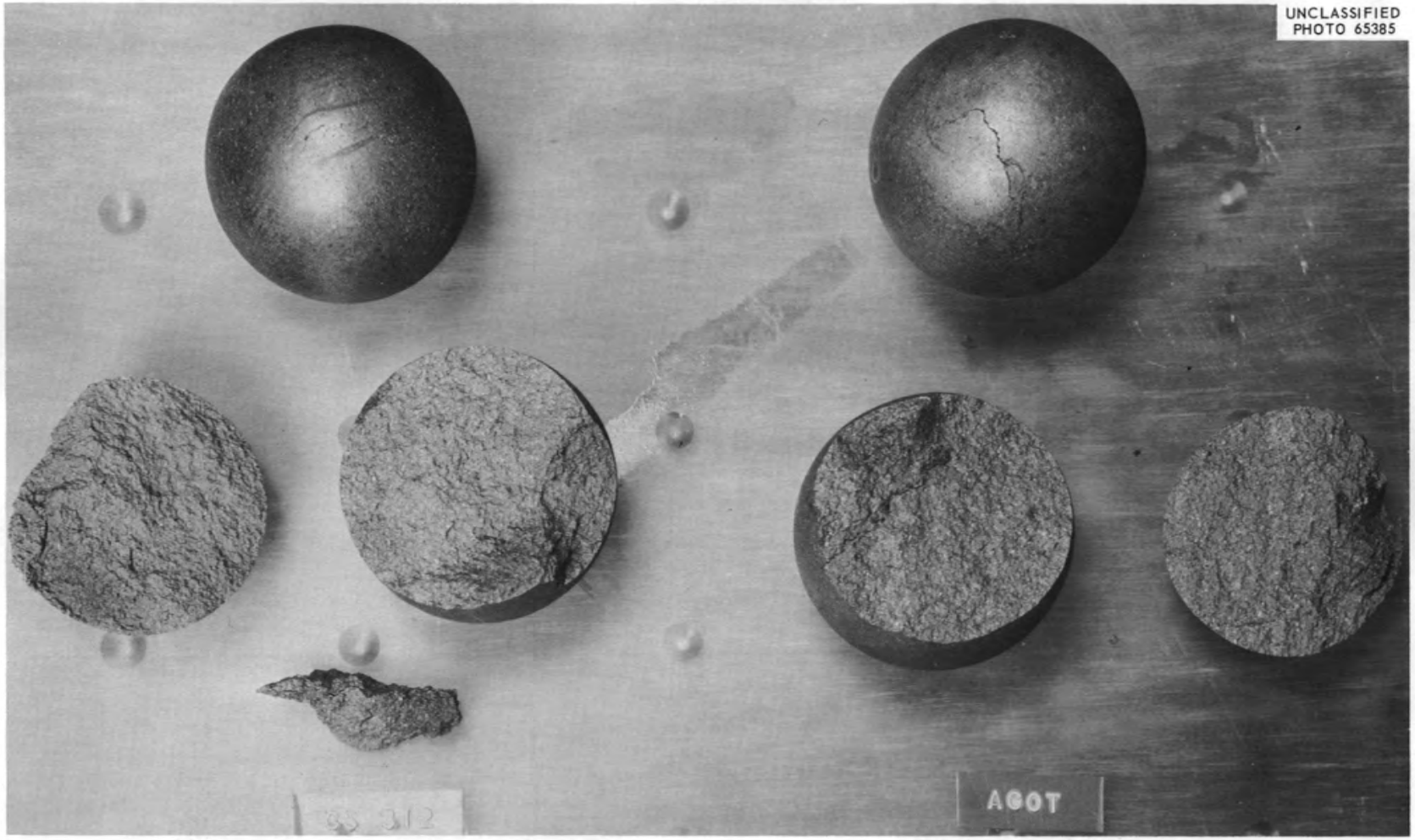

Fig. 40. Typical Failures in 6-cm-diam Graphite Spheres Dropped from 13 m onto a Steel Plate. Left: Grade CS-312. Right: Grade AGOT.

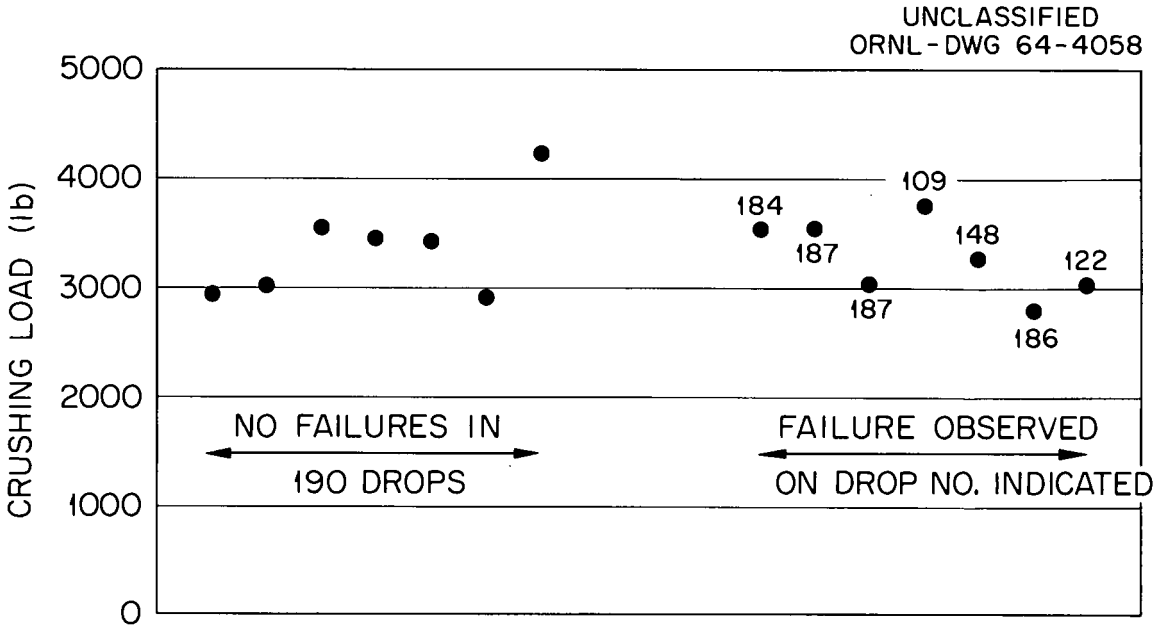

Fig. 41. Crushing Load of 1 1/2-in.-diam Spheres of ATJ Graphite Machined Concentrically from 6-cm-diam Spheres After Dropping from 5 m with Random Orientation onto Steel Plate.

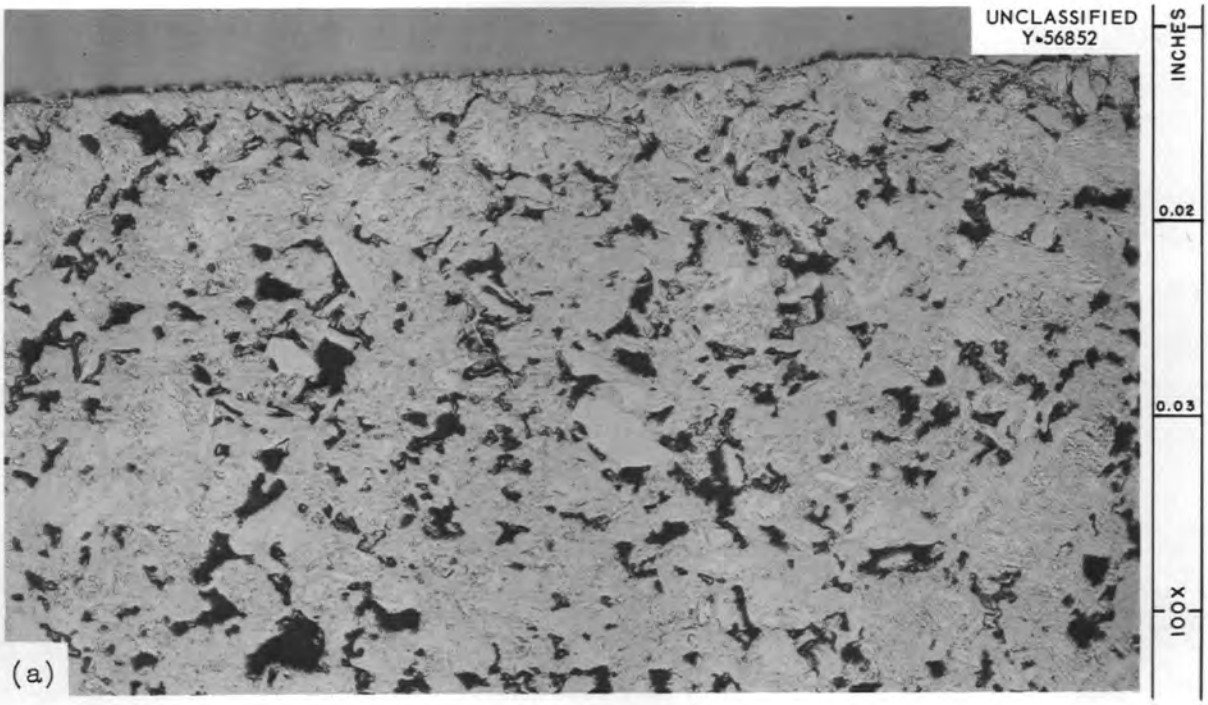

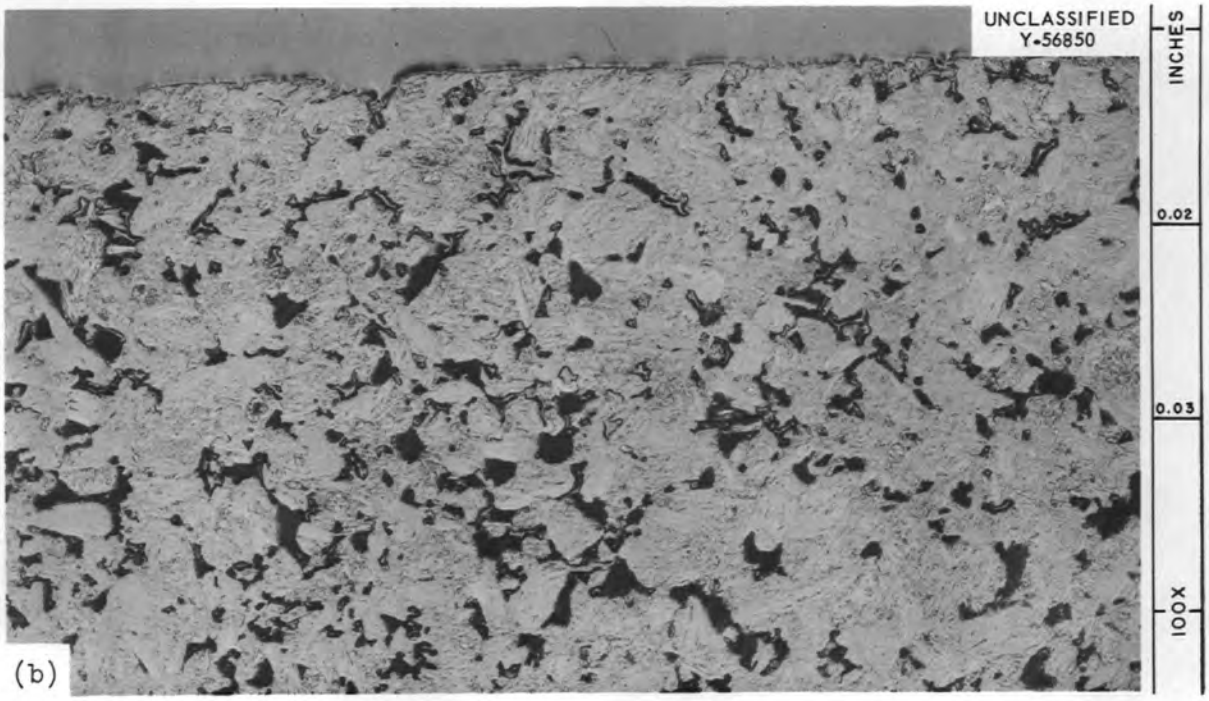

Fig. 42. Microstructure of ATJ Graphite. (a) Region of impact after dropping onto steel plate from 27.3 m. As polished. (b) Region diametrically opposite impact region in (a) above. As polished.

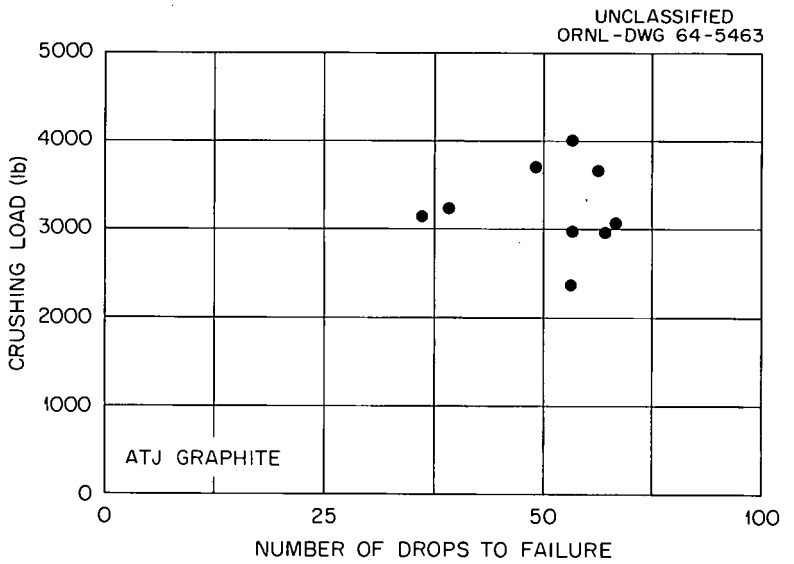

Fig. 43. Crushing Load of 1 1/2-in.-diam Spheres Machined Concentrically from 6-cm-diam Spheres After Failure in Free-Drop Tests from 13 m with Random Orientation onto Steel Plate.

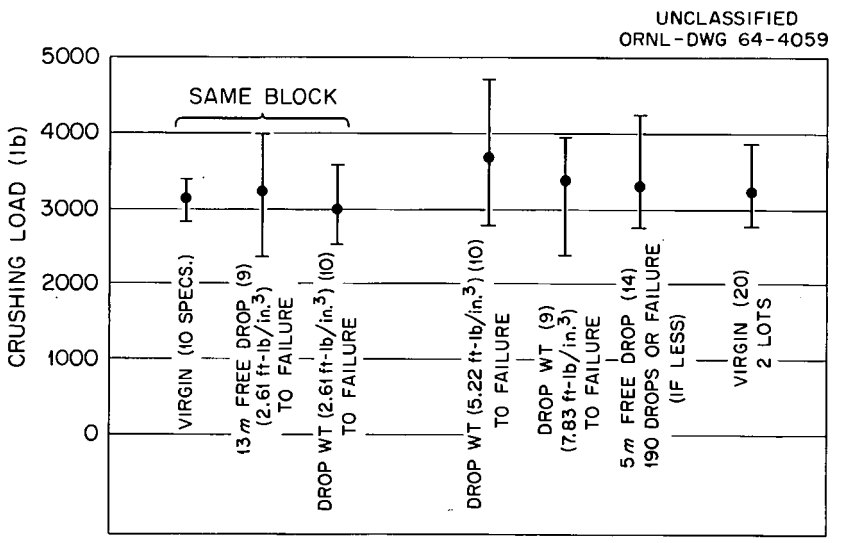

Fig. 44. Crushing Strength of 1 1/2-in.-diam Spheres Machined from Virgin Stock or Concentrically from 6-cm-diam Spheres After Free Drop on Steel Plate or Drop-Weight Tests; ATJ Graphite.

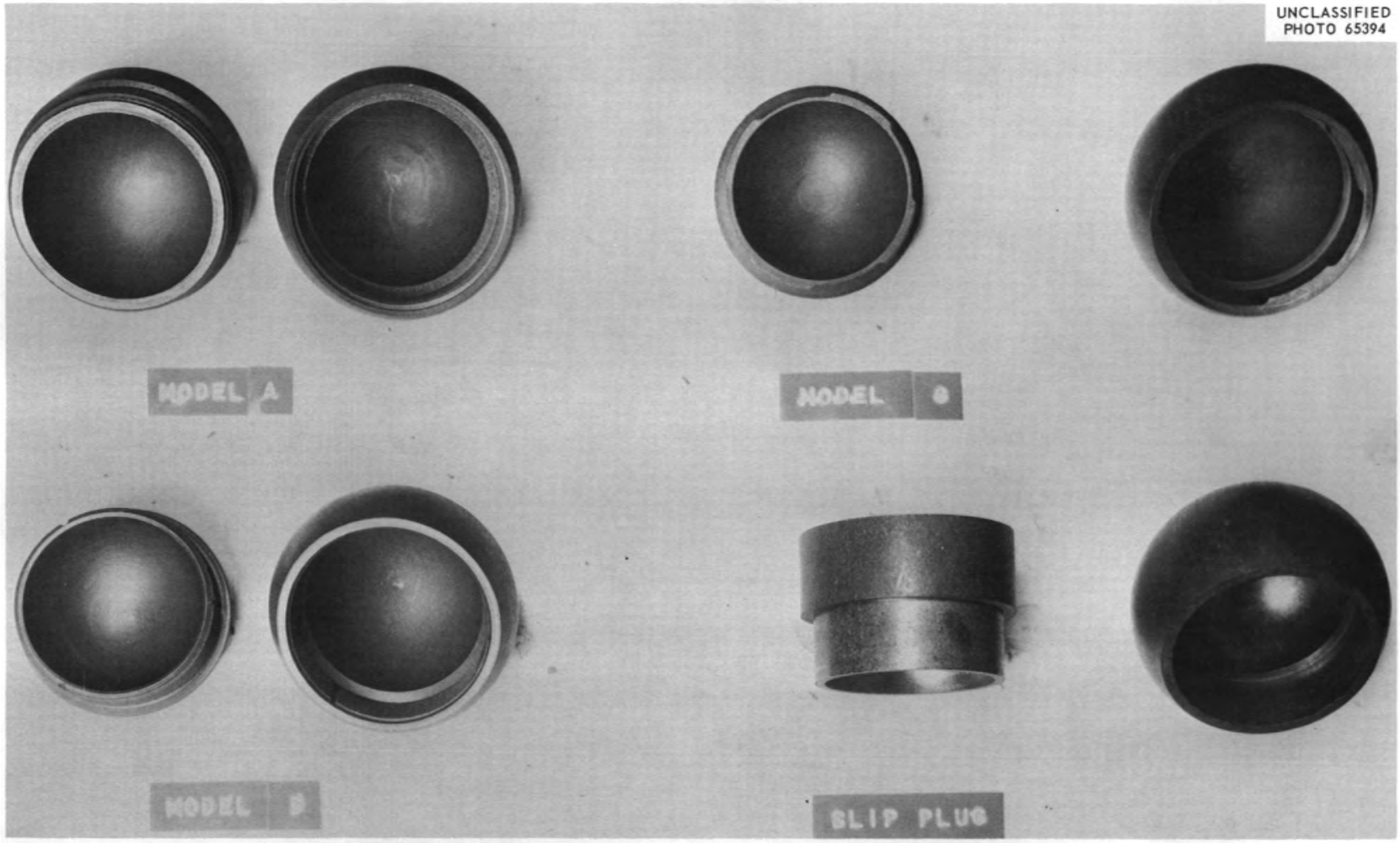

Fig. 45. Four Shell Models Before Assembly.

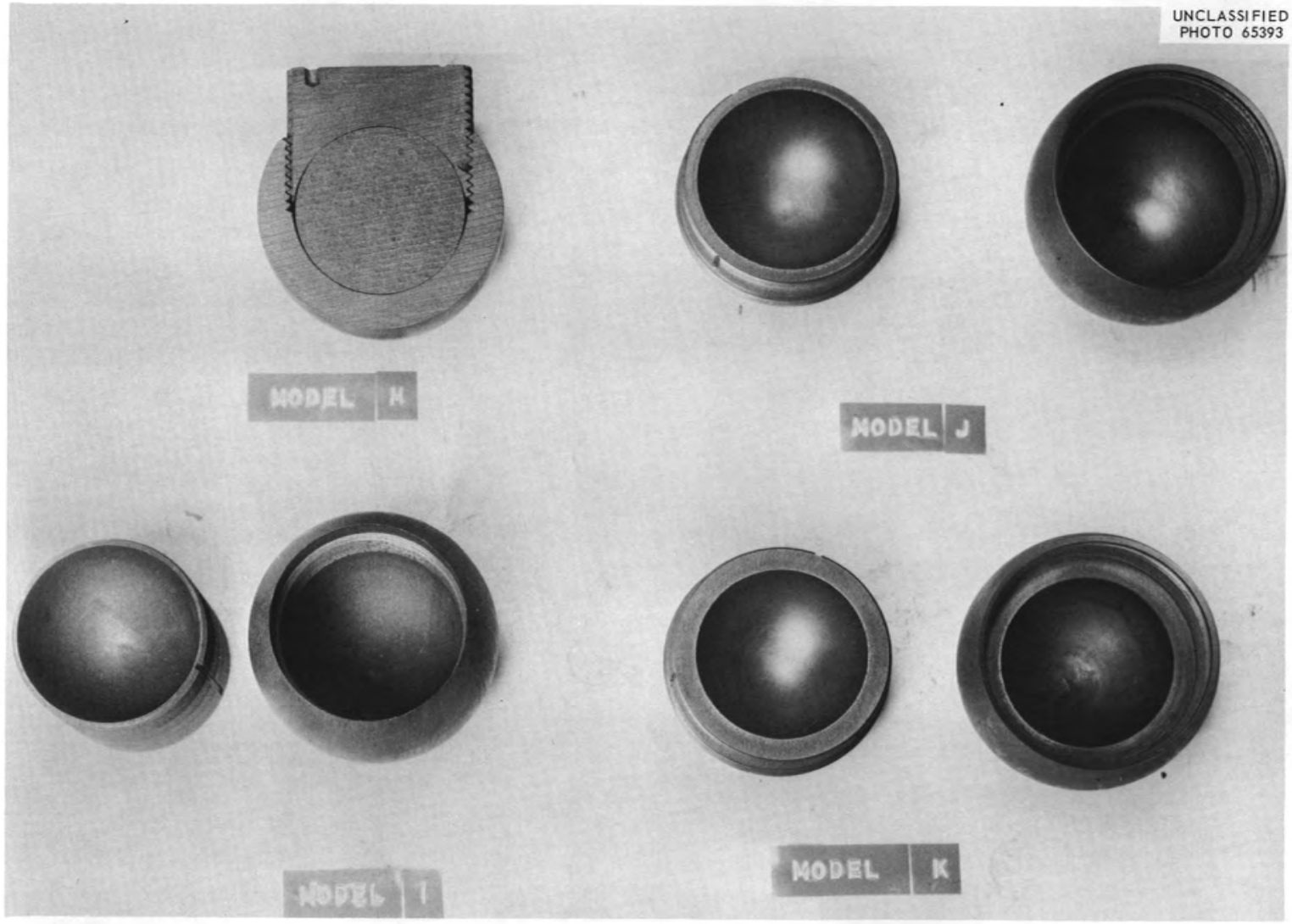

Fig. 46. Four Shell Models Before Assembly.

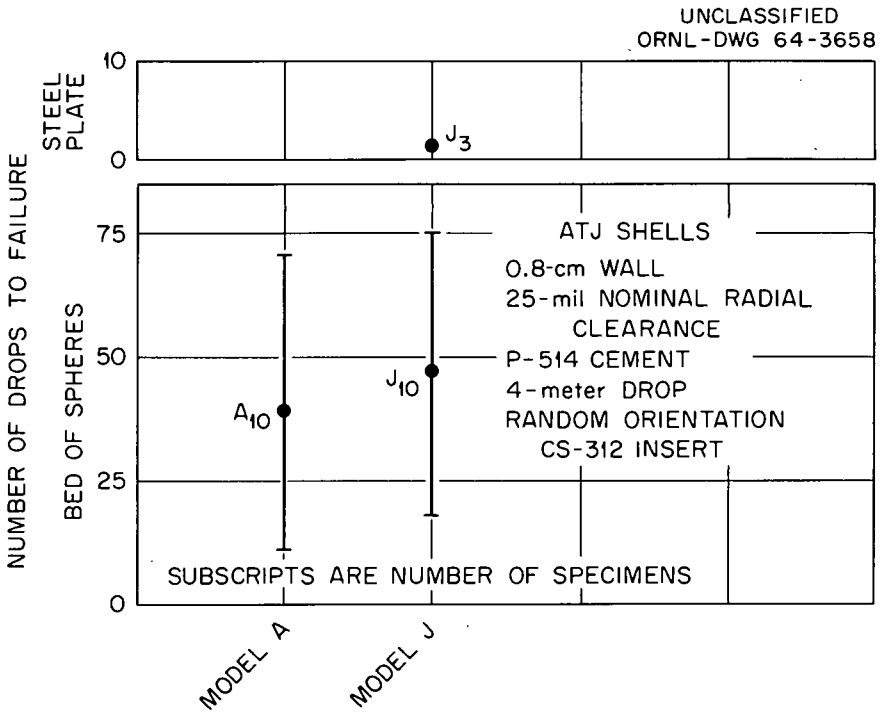

Fig. 47. Comparison of Number of Drops for Failure in Free-Drop Tests of Various Shell Models.

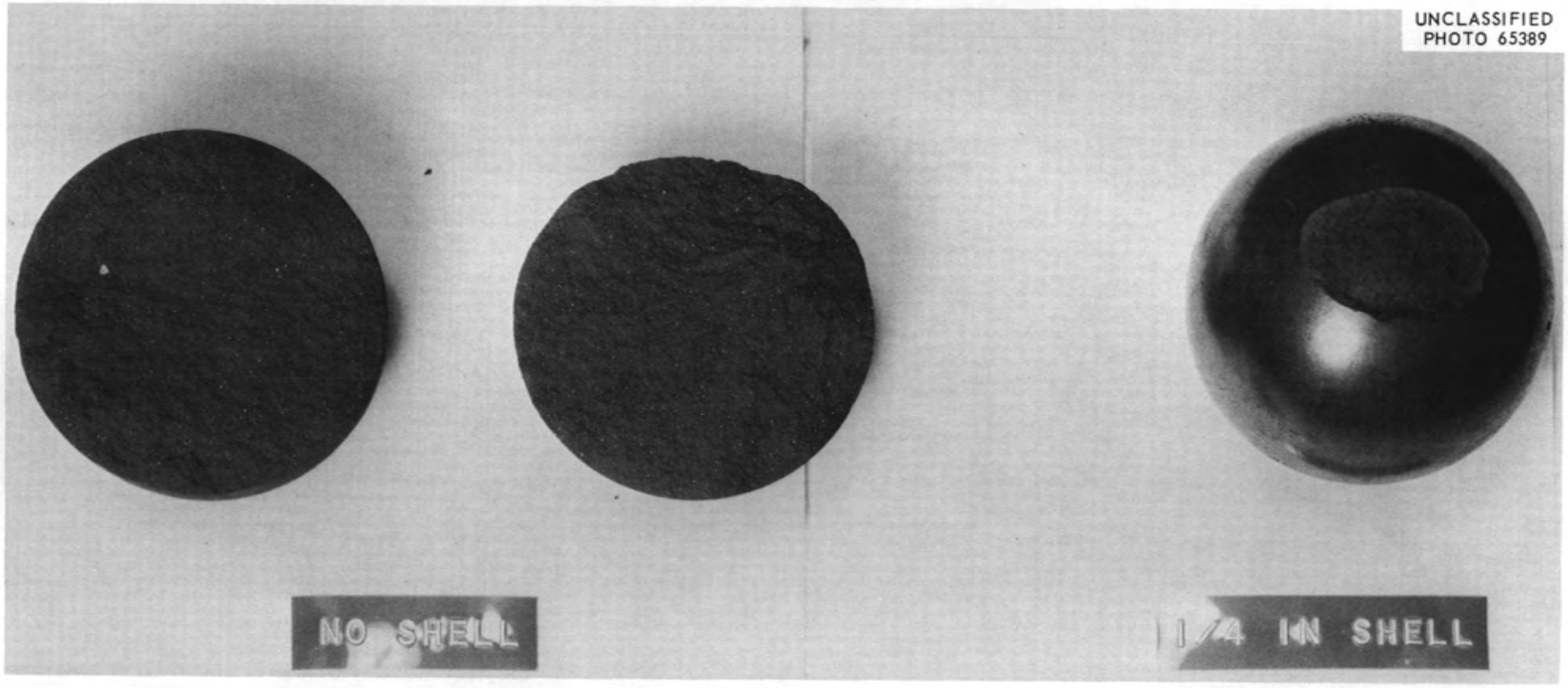

Fig. 48. Failures in All-Molded Fueled Spheres (3M) in Free-Drop Tests (See Table 3).

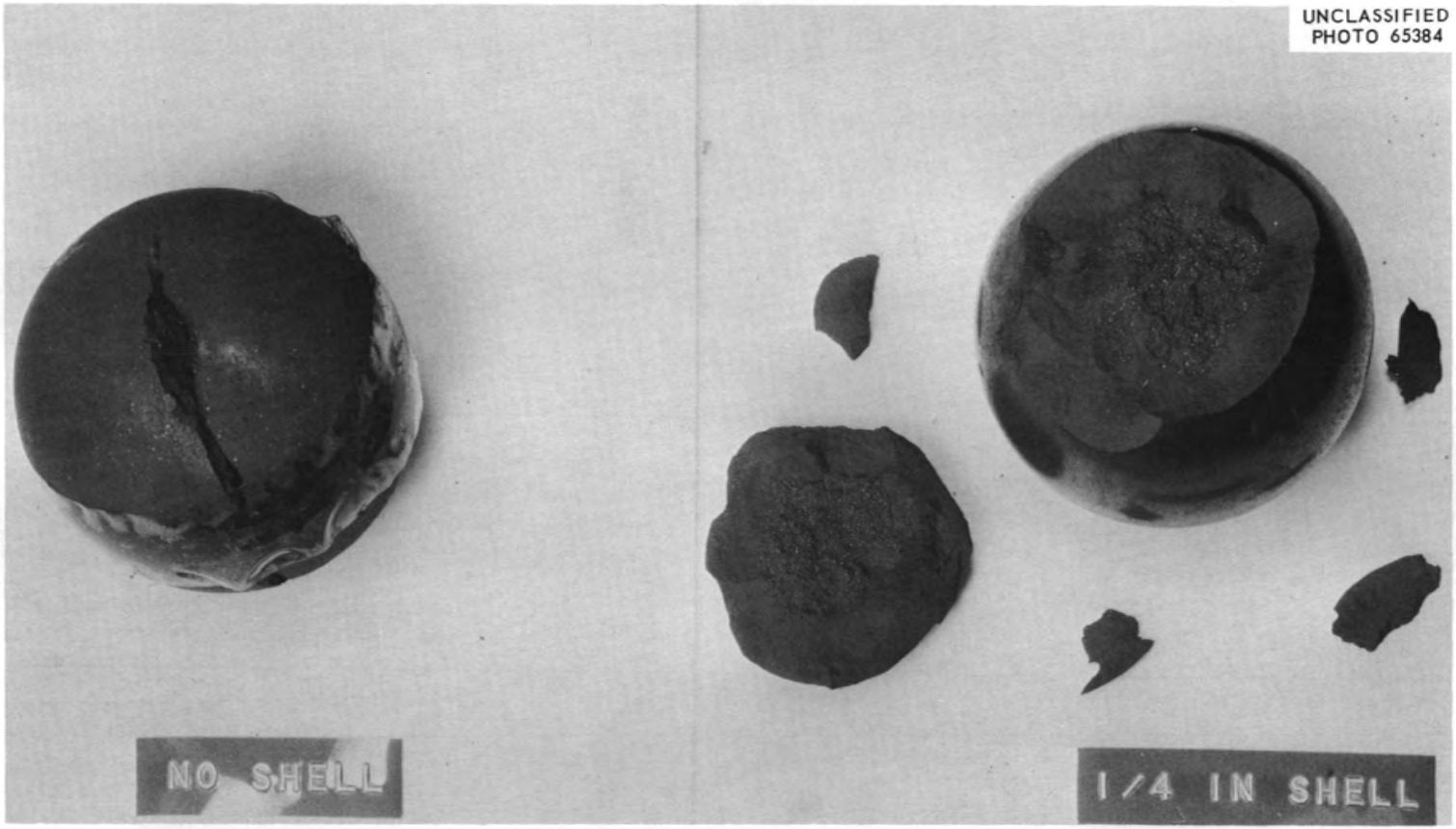

Fig. 49. Failures in All-Molded Fueled Spheres (3M) After Thermal Cycling in Free-Drop Tests (See Table 3).

Table 4. Results of Free-Drop Tests of Simulated AVR Fuel Elements, 6-cm-diam and 0.8-cm-thick-wall ATJ Graphite Shells, CS-312 Inserts

Model Type	Nominal Radial Clearance (mils)	Cement Used	Portion Cemented	Ultrasonic Cleaning	Closure Torque (in.-lb)	Number of Specimens	Number of Drops for Failure from 4 m: Onto Bed of Spheres			Onto Steel Plate		
							Minimum	Average	Maximum	Minimum	Average	Maximum
A	5	P-514	All	Yes	15	5		75[a]		1	3.6	7
A	5	P-514	All	No	15	5		75[a]		1	4.2	10
A	5	P-514	All	No	50	5		75[a]		3	6.8	15
A	5	P-514	Threads only	No	15	5	10	24.6	32			
A	5	P-514	Threads only	No	60	5	19	38.0	47			
A	25	P-514	All	Yes	15	5	11	39.8	71			
A	25	P-514	All	No	15	5	31	39.0	48			
A	40	P-514	All	Yes	15	10	11	23.0	41			
A	40	P-514	All	Yes	70	5	3	25.2	44			
A	40	C-10	All	Yes	15	5	22	29.6	52			
A	40	P-514	Threads only	Yes	15	5	3	6.8	12			
B[d]	5	P-514	All	No	b	15	63	74.2[c]	75	1	1.9	5
B[d]	5	P-514	All	No	b	10	6	48.0[d,e]	75	1	3.2	7
B[d]	40	P-514	All	No	b	5	10	18.8	26			
B[d]	40	P-514	All	No	b	5	5	19.4	27			
G	5	P-514	All	Yes	f	4	39	47.5	58			
G	40	P-514	All	Yes	f	4	1	5.2	11			
H	40	P-514	All	No	15	5	75	75[e]	75	2	4.8	7
I_1	5	P-514	All	No	15	7		75[a]		2	2.3	3
I_2	5	P-514	All	No	15	5	9	33.6[g]	75		1	
I_2	5	P-514	All	No	30	5	6	27.2[g]	75		3	
I_2	25	P-514	All	No	15	5	4	22.0	29			
I_2	25	P-514	All	No	30	11	3	34.0[h]	75		1	
I_1	40	P-514	All	No	15	5	51	70.2[i]	75	1	1.7	3
I_1	40	P-514	All	No	30	6		75[a]		1	2.7	7
I_2	40	P-514	All	No	15	5	11	23.2	50			
I_2	40	P-514	All	No	30	7	10	31.9[g]	75		1	

Table 4 (continued)

Model Type	Nominal Radial Clearance (mils)	Cement Used	Portion Cemented	Ultrasonic Cleaning	Closure Torque (in.-lb)	Number of Specimens	Number of Drops for Failure from 4 m: Onto Bed of Spheres			Onto Steel Plate		
							Minimum	Average	Maximum	Minimum	Average	Maximum
J	5	P-514	All	No	b	10		75[a]		1	3.0	7
J	25	P-514	All	No	b	10	18	47.5[i]	75	1	1.7	2
J	25	Hexalon	All	No	b	9	9	45.7[i]	75		1	
J[j]	25	P-514	All	No	b	10	20	50.8[g]	75		1	
J	40	P-514	All	No	b	10	11	18.1	32			
K[k]	5	P-514	All	No	b	10		75[a]		1	4.4	12
K[k]	25	P-514	All	No	b	9	65	73.9[ℓ]	75	1	1.2	2
K[k,j]	25	P-514	All	No	b	9	66	74.0[ℓ]	75	1	1.4	3
K[k]	40	P-514	All	No	b	10	31	68.6[ℓ]	75	1	1.2	2

[a] All specimens survived without failure.
[b] Not measured.
[c] Fourteen specimens survived without failure.
[d] AGOT graphite shell.
[e] Four specimens survived without failure.
[f] Torque not required.
[g] One specimen survived without failure.
[h] Two specimens survived without failure.
[i] Three specimens survived without failure.
[j] After 10 thermal cycles.
[k] Wall 1 cm thick.
[ℓ] Eight specimens survived without failure.

ORNL-3723
UC-25 — Metals, Ceramics, and Materials
TID-4500 (36th ed.)

INTERNAL DISTRIBUTION

1-3. Central Research Library
4. Reactor Division Library
5-6. ORNL — Y-12 Technical Library
Document Reference Section
7-26. Laboratory Records Department
27. Laboratory Records, ORNL R.C.
28. ORNL Patent Office
29. E. S. Bomar
30. F. L. Carlsen, Jr.
31. J. H. Coobs
32. D. R. Cuneo
33. J. E. Cunningham
34. C. V. Dodd
35. J. H Frye, Jr.
36. T. G. Godfrey
37. A. E. Goldman
38-42. W. O. Harms
43-47. M. R. Hill
48. C. E. Larson
49. C. F. Leitten, Jr.
50. H. G. MacPherson
51. H. C. McCurdy
52. S. E. Moore
53. M. F. Osborne
54. P. Patriarca
55-59. J. M. Robbins
60. M. W. Rosenthal
61. G. Samuels
62. H. W. Savage
63. J. L. Scott
64-68. C. O. Smith
69. J. E. Smith
70-113. D. B. Trauger
114. A. M. Weinberg
115. F. J. Witt
116. G. T. Yahr
117. M. B. Bever (consultant)
118. A. A. Burr (consultant)
119. J. R. Johnson (consultant)
120. A. R. Kaufmann (consultant)

EXTERNAL DISTRIBUTION

121. C. M. Adams, Jr., Massachusetts Institute of Technology
122. H. C. Brassfield, General Electric Company, NMPO
123. M. N. Burkett, Carbon Products Division, Lawrenceburg
124-125. D. F. Cope, AEC, Oak Ridge Operations Office
126. W. V. Goeddel, General Atomic
127. J. L. Gregg, Bard Hall, Cornell University
128. W. D. Manly, Union Carbide Corporation, New York
129. J. Simmons, AEC, Washington
130. E. E. Stansbury, University of Tennessee
131. D. K. Stevens, AEC, Washington
132. J. F. White, General Electric Company, NMPO
133. Research and Development Division, AEC, ORO
134-638. Given distribution as shown in TID-4500 (36th ed.) under Metals, Ceramics, and Materials category